Detailed Spectroscopic Study of Light-to-Heavy Λ-hypernuclei

--encouraging HIHR projects from (personal) history--

11 December 2021, Sendai

Toshio MOTOBA

(Osaka E-C University)

京大基研協同研究員, 阪大RCNP協力研究員

理研客員研究員

0. Introduction

From an old drawings, Figures appeared in Nucl. Phys. A**547** (1992) 379c.
Hyp. Conference held in Shimoda (1991).

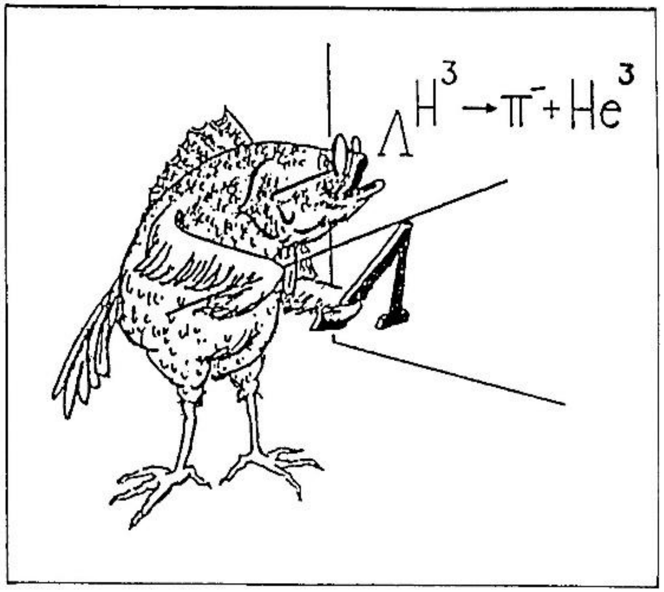

Fig.3 *"Neither fish nor fowl ? "* as drawn by Bea Pace. Taken from Ref.[19]

[19] Proc. Int. Conf. on Hypernuclear Physics (Argonne 1969)

"Hypernuclear Physics is in a strange position. It is neither fish nor fowl. High energy physicists do not look it for valuable advances in their understanding of the interactions of fundamental particles. Nuclear physicists also see the fields as something apart. It main relevance for fundamentals is the information it can provide on N-Λ and Λ-Λ interactions……"

(from a book review by J.D. Jackson, SCIENCE **158**, 3821 (1968), p.1346.)

hyperon many-body systems

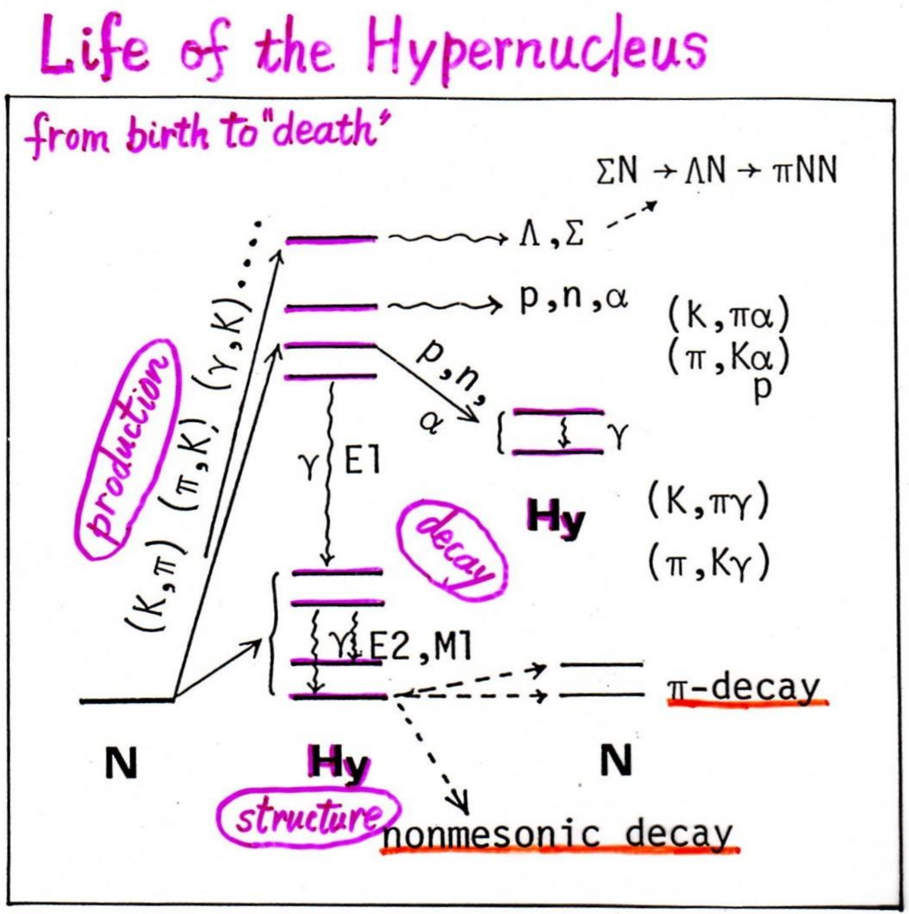

Philosophy: Production, Structure, and Decays as a whole

● First chart in cubic axes

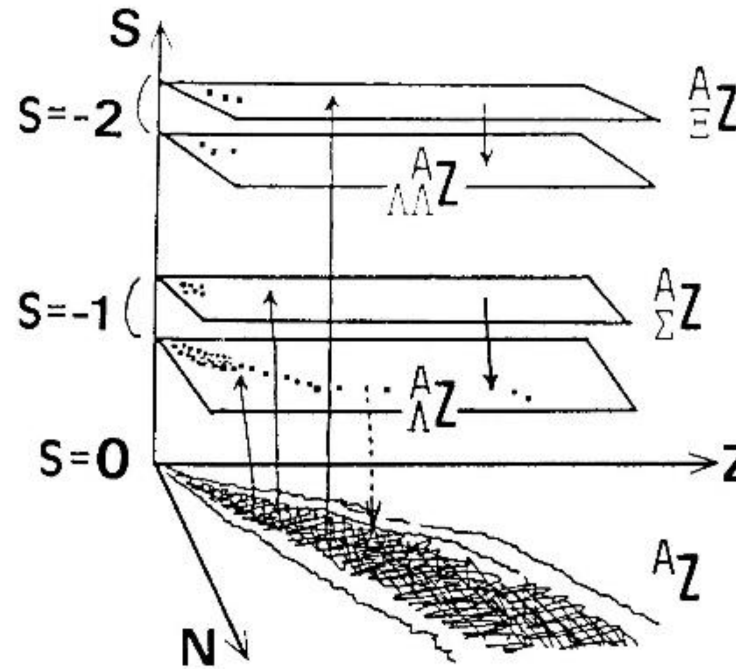

Fig. 8 Hypernuclei and ordinary nuclei in the $\{N, Z, S\}$ cubic axes[30].

T. Motoba, NPA **547** (1992) 379c;
First: Genshikaku Kenkyu **32** (1987) 97 (大ハドロン計画シンポジウム).

INS symp. (1995) *Nuclear and Particle Physics with Meson beams in the 1 GeV/c Region*

(2001) *Physics of GeV Electrons and Gamma-Rays*

SENDAI 03: *Electrophotoproduction of Strangeness on Nucleons and Nuclei*

SENDAI08: *Strangeness in Nuclear and Hadronic Systems*

There have been good collaborations between experimentalists and theorists.

Roles of theory sides:

(1) Predictions (rough or detailed)

(2) Interpretation or consistent understanding of exp. data

(3) Characteristics of different (virtual) prod. reactions

CONTENTS

(1) Introduction

(2) Predictions of $^{89}\mathbf{Y}(\pi+,K+)\ {}_{\Lambda}^{89}\mathbf{Y}$ and theoretical interpretation after the experiment

(3) Interplay of a hyperon and nuclear core dynamics (Sm isotopes, 9Be, 13C)

(4) Comments on suitable (preferable) targets

(2) Prediction of ^{89}Y(π+,K+) $_{\Lambda}^{89}$Y and theoretical interpretation after the experimental spectrum

- Targets: 9Be, 12C, 28Si, 56Fe, 89Y, 208Pb, ETC.
- Theory:

C.B. Dover, L. Ludeking and G.E. Walker, Phys. Rev. C **22**, 2073 (1980).

H. Bando and T. Motoba, Prog. Theor. Phys. **76**, 1321 (1086).

T. Motoba, H. Bando, R. Wuensch, and J. Zofka, Phys. Rev. C **38**, 1322 (1988).

ETC.

- EXP

BNL: R.E. Chrien group ……….

T. Hasegawa, et al. , PRL **74**, 224 (1995); Phys. Rev. C **53**, 1210 (1996).

H. Hotchi, et al., Phys. Rev. C **64**, 044302 (2001).

Low partial waves are more reduced by absorption effect, leading to high-L role enhancement

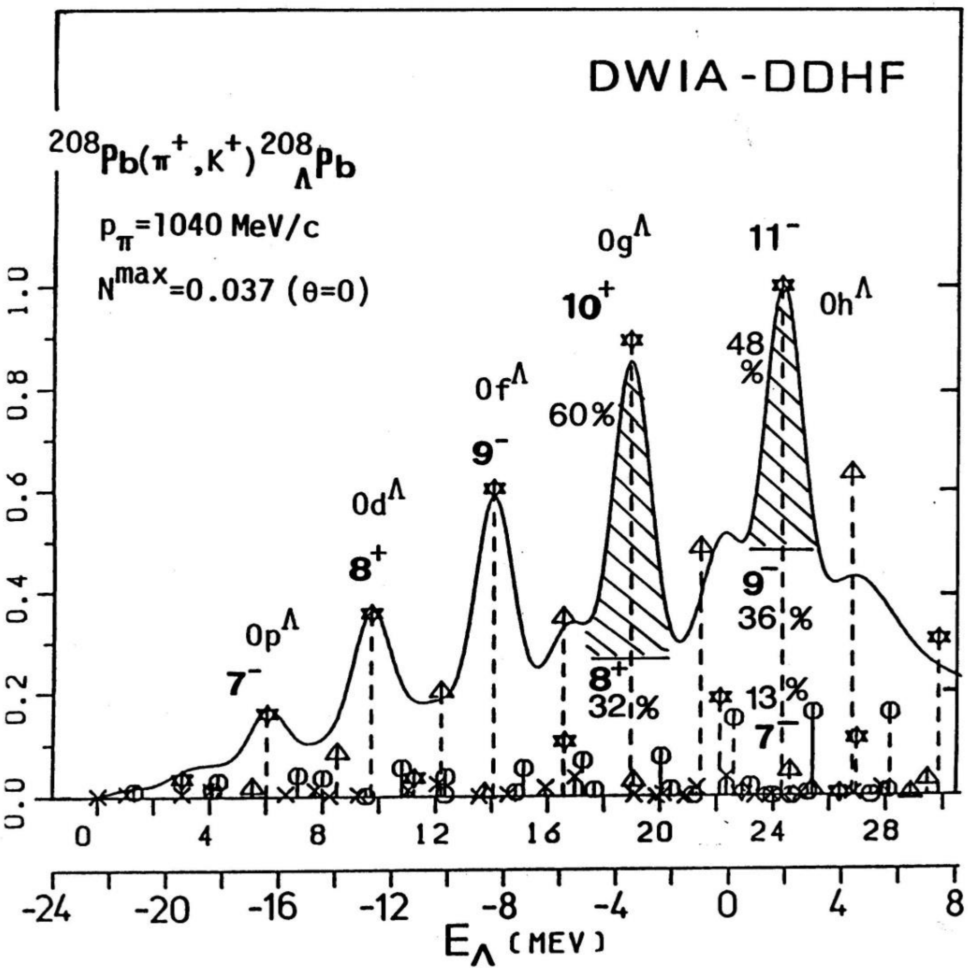

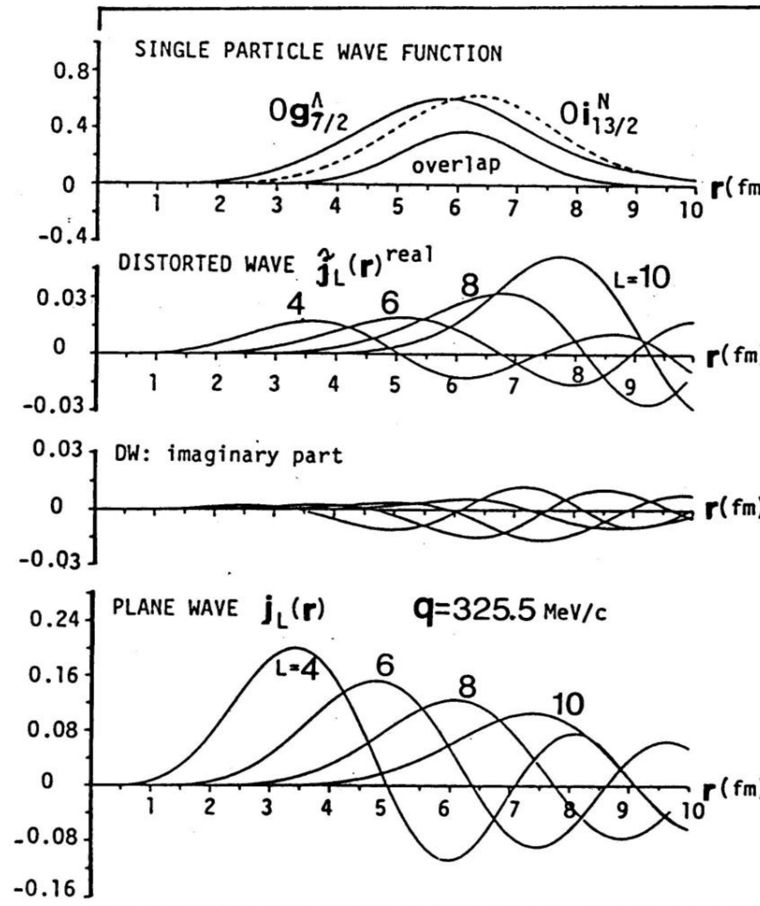

Hyperon recoil momentum and the transition operator determine the reaction characteristics

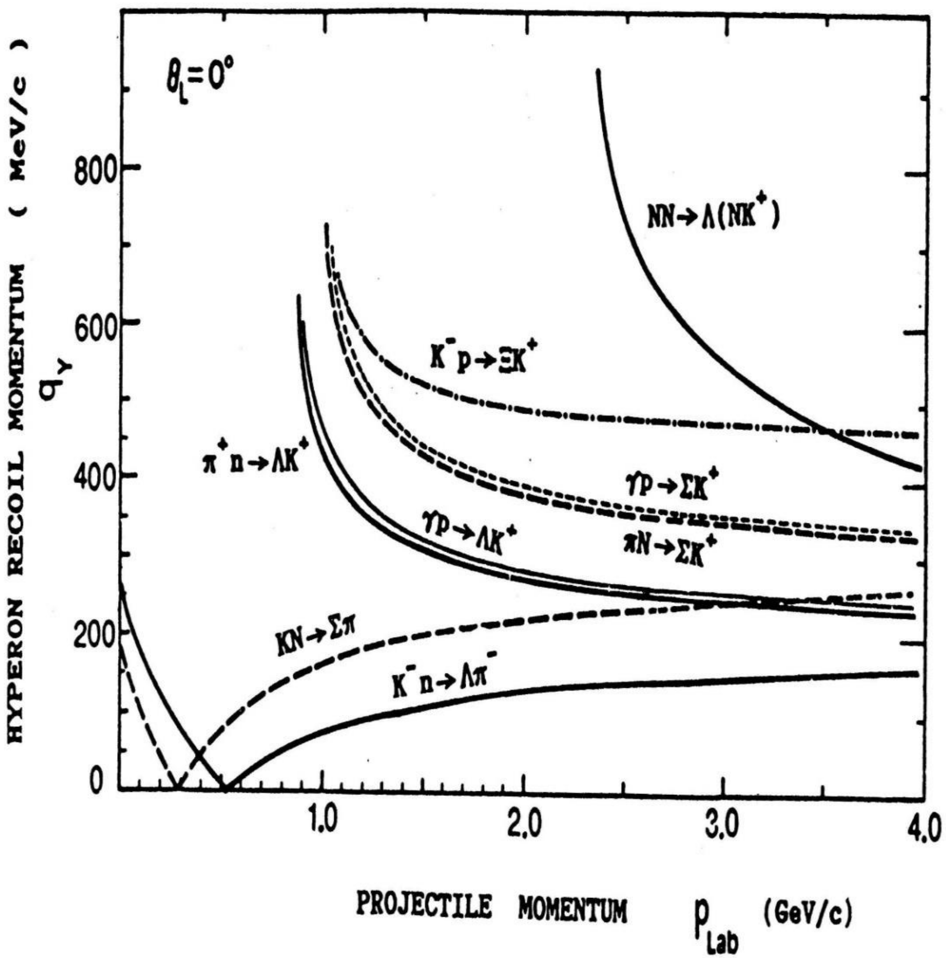

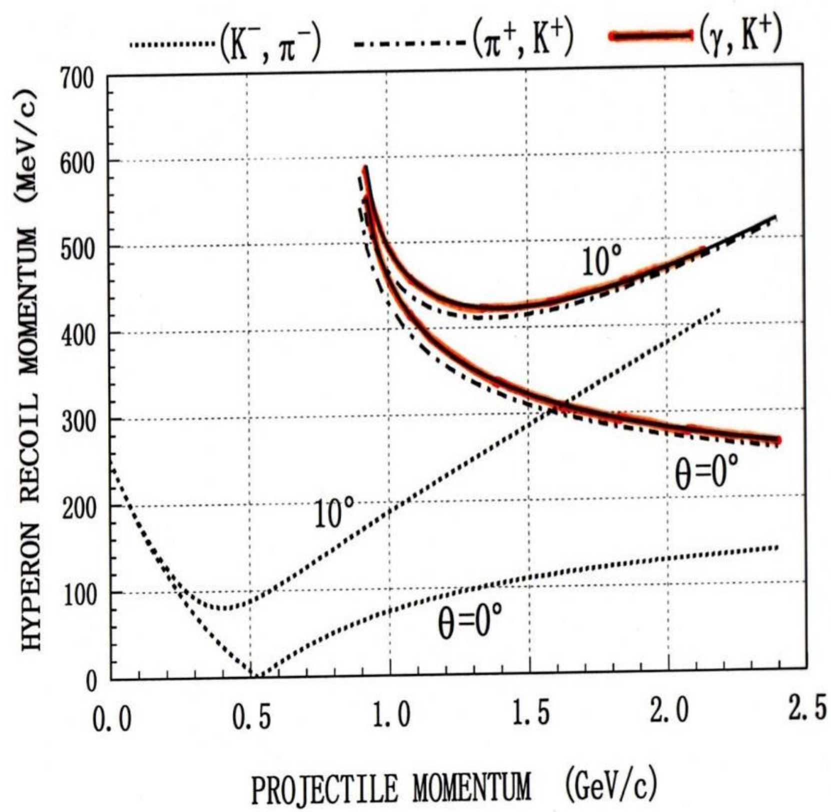

q_Λ**=350-420** MeV/c at Eγ=1.3 GeV

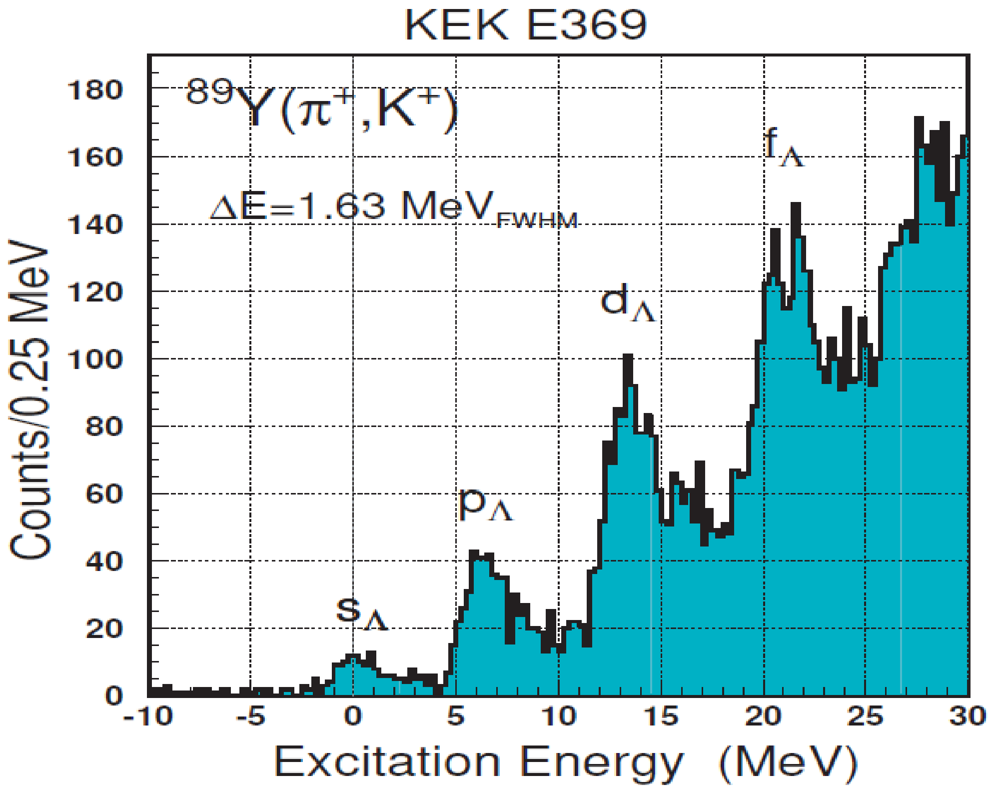

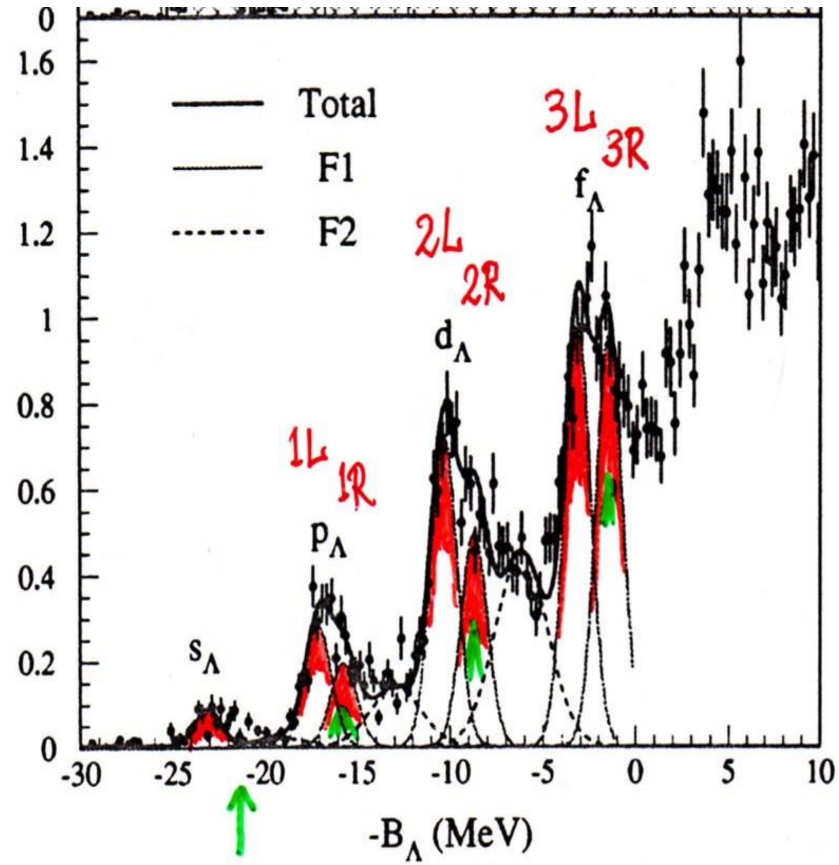

H. Hotchi et al., Phys. Rev. C 64, 044302 (2001)

Great achievement as a "Textbook example"

BUT

we had a serious discrepancy between the prediction and the exp. and how to understand the doublet-like peaks:

Figure from Bohr-Mottelson textbook

§ 2-4 AVERAGE NUCLEAR POTENTIAL 239

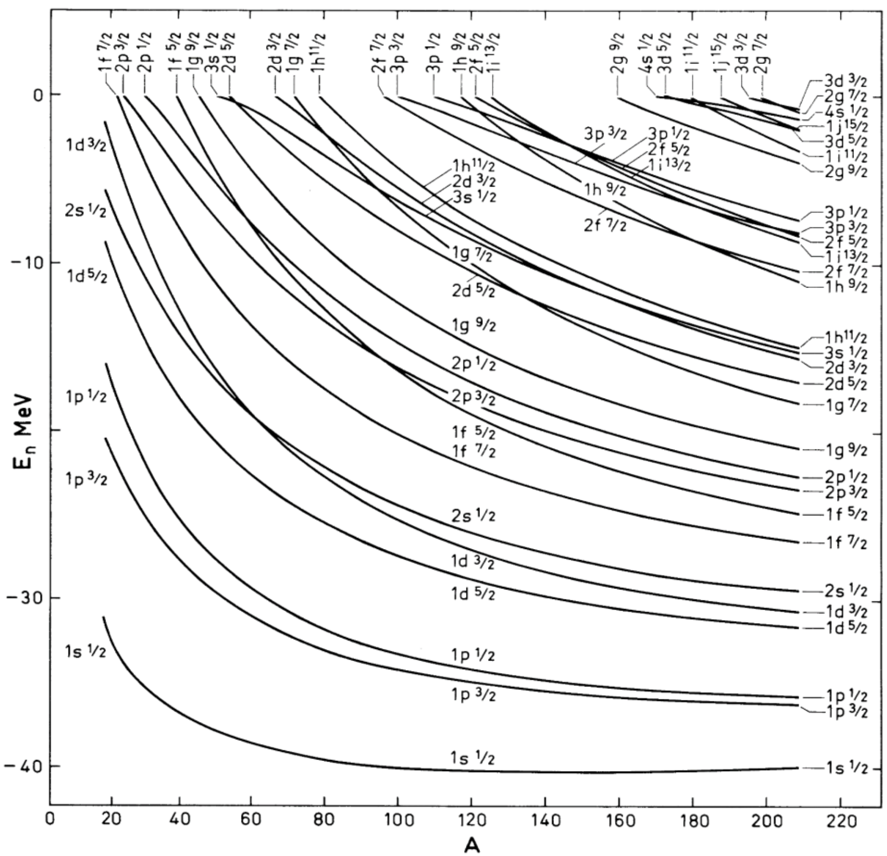

Figure 2-30 Energies of neutron orbits calculated by C. J. Veje (private communication).

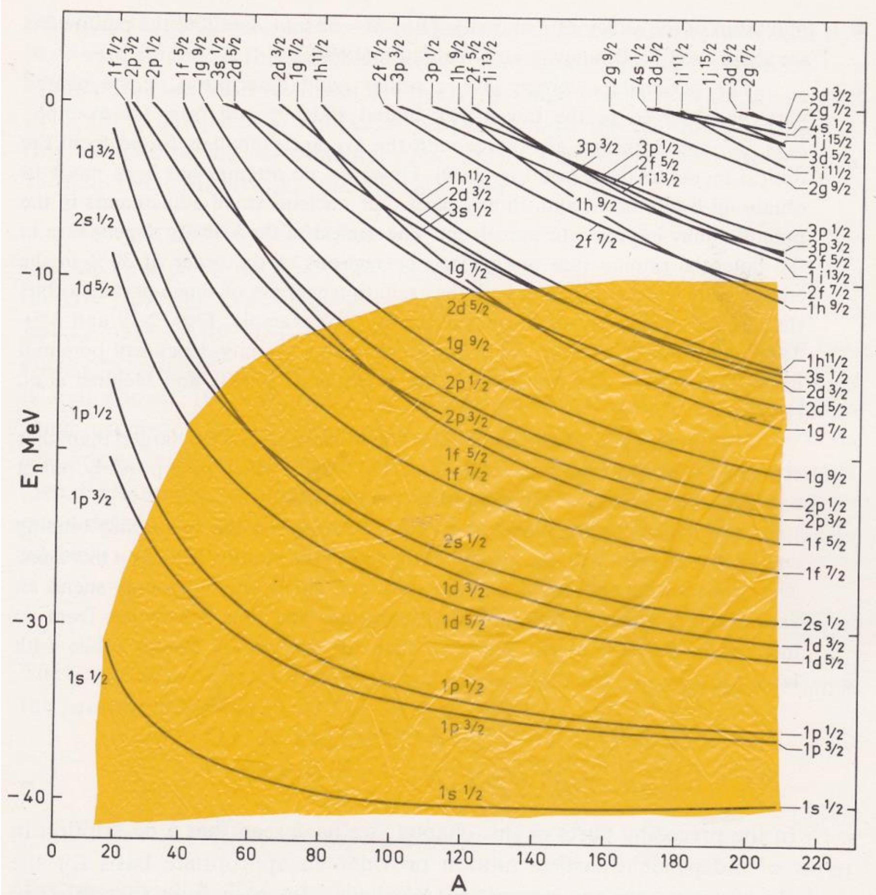

Figure 2-30 Energies of neutron orbits calculated by C. J. Veje (private communication).

Note: The shaded part cannot be accessed because of the too large spreading widths for nucleon-hole states. OK for hyperon!

How to understand "large" splitting of subpeaks observed in heavy systems

3) High-precision γ ray measurements in $^{7}_{\Lambda}Li$, $^{9}_{\Lambda}Be$, $^{13}_{\Lambda}C$ clearly confirmed

very small spin-orbit ΛN interaction.

↓

How to understand the doublet-like subpeaks observed in medium-heavy hypernuclei ?

spin-orbit splitting or other origins ?

ΔE is not proportional to (2l+1)

If we assume that each doublet corresponds to $j_>$ and $j_<$,

Two Serious problems arise:

(1) Energy splittings are not proportional to $(2\ell+1)$.

Peaks		E_Λ (MeV)	ΔE_Λ	(ΔE_Λ ratio) (EXP)	(HO)	(WS-CAL)
ℓ=0		−23.11				
ℓ=1	L	−17.10	1.37	(1.0)	(1.0)	(1.0)
	R	−15.73				
ℓ=2	L	−10.32	1.63	(1.19)	(1.67)	(2.16)
	R	−8.69				
ℓ=3	L	−3.13	1.70	(1.24)	(2.33)	(3.36)
	R	−1.43				

If we assume that each doublet corresponds to $j_>$ and $j_<$,

Two Serious problems arise:

(2) Cross section ratio is opposite to the theory .

Peaks		E_Λ (MeV)	σ (μb/sr)	L/R ratio (EXP)	L/R ratio (DWIA-CAL)
ℓ=0		−23.11	0.60		
ℓ=1	L	−17.10	2.00	} 1.45	1.00 (L=R)
	R	−15.73	1.38		
ℓ=2	L	−10.32	5.10	} 1.45	0.55 (L<R)
	R	−8.69	3.52		
ℓ=3	L	−3.13	6.87	} 1.01	0.44 (L<R)
	R	−1.43	6.79		

XS ratio is determined in DWIA as

DW: Solve Klein-Gordon Eq for π and K partial waves.

$$O = \chi_K^{(+)*}(r)\chi_\pi^{(-)}(r) = \sum_{\kappa}\sum_{\mu}\sqrt{[4\pi(2\kappa+1)]}\, i^\kappa\, \tilde{j}_{\kappa\mu}(\theta;r)\, Y_{\kappa\mu}(\Omega)$$

$d\sigma/d\Omega$ for $[j_n^{-1} j_\Lambda]_J$ p-h state is proportional to

$$(2j_\Lambda+1)(2j_n+1)(j_\Lambda 1/2\, j_n -1/2 | J0)^2 \left|\langle j_\Lambda | \tilde{j}_{\kappa\mu}(\ ) | j_n \rangle\right|^2$$

$jn=g9/2=l+1/2$ ------→ $j\Lambda=l-1/2$ ($f5/2$) larger XS

------→ $j\Lambda=l+1/2$ ($f7/2$) less

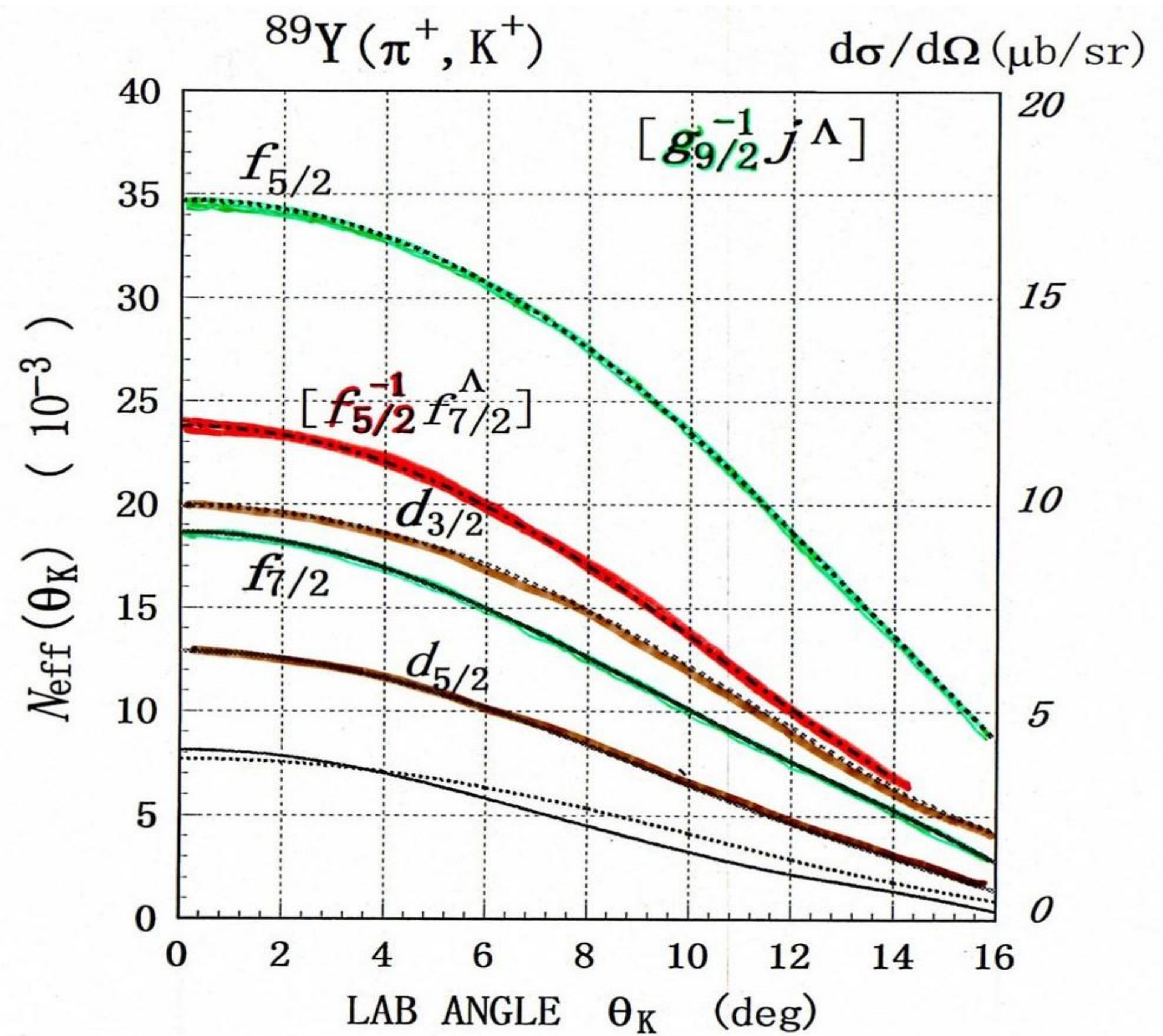
89Y (π+, K+)
dσ/dΩ (μb/sr)
[g9/2−1 jΛ]
f5/2
[f5/2−1 f7/2Λ]
d3/2
f7/2
d5/2
Neff (θK) (10−3)
LAB ANGLE θK (deg)
40
35
30
25
20
15
10
5
0
20
15
10
5
0
0
2
4
6
8
10
12
14
16

EXP(2001) vs. DWIA CAL (1988) V_{LS}=4.3MeV

j=*l*+1/2 seems stronger in EXP, but CAL is opposite.

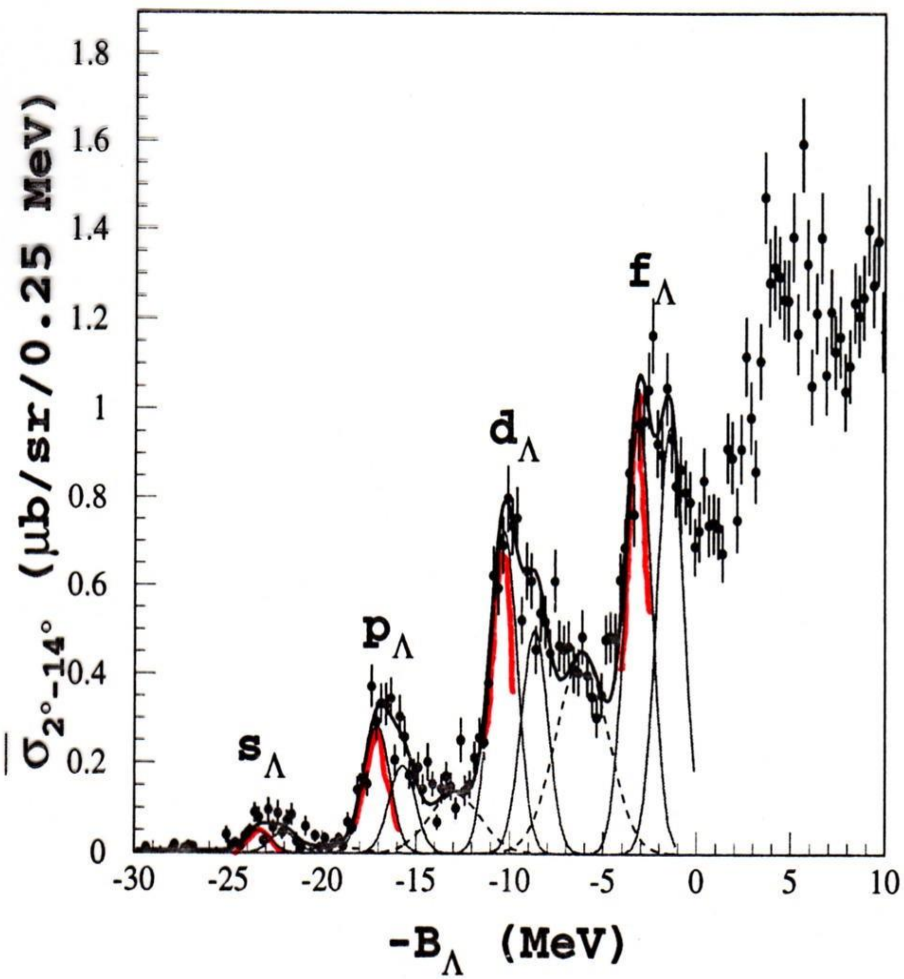

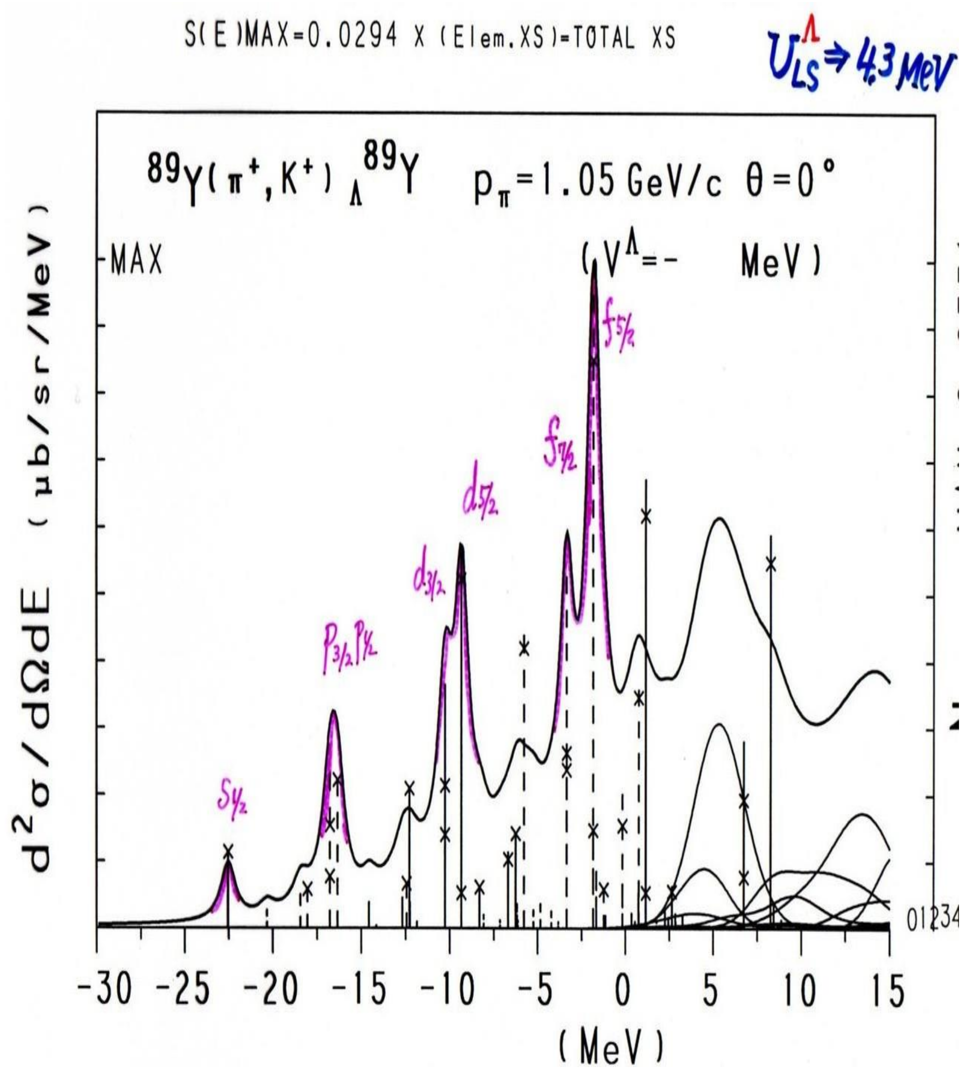

Models for Stucture of $^{89}{}_{\Lambda}Y$:

Shell model analysis

(1) The simplest model with 1-hole core
(assume a ^{90}Zr target)

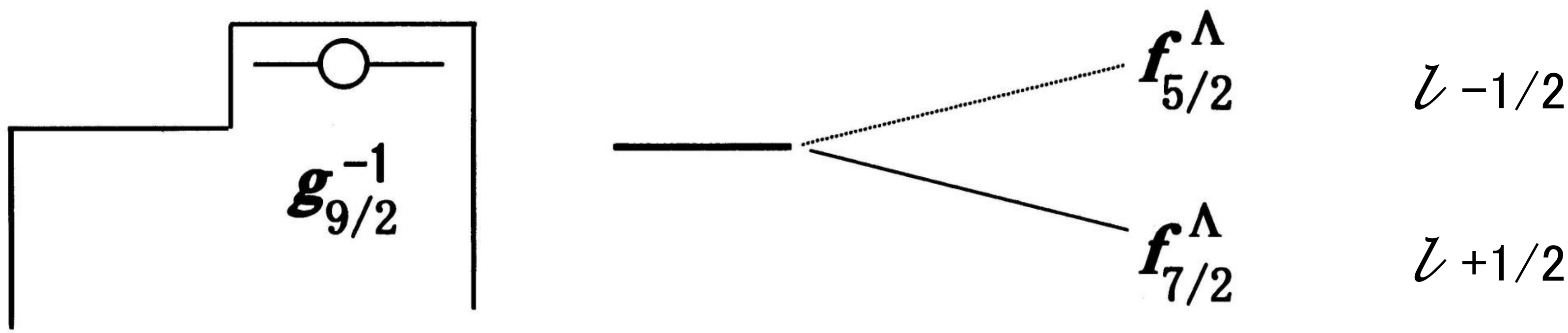

(2) Role of an odd proton introduced
(single 1p-1h core): 2 levels in ^{88}Y.

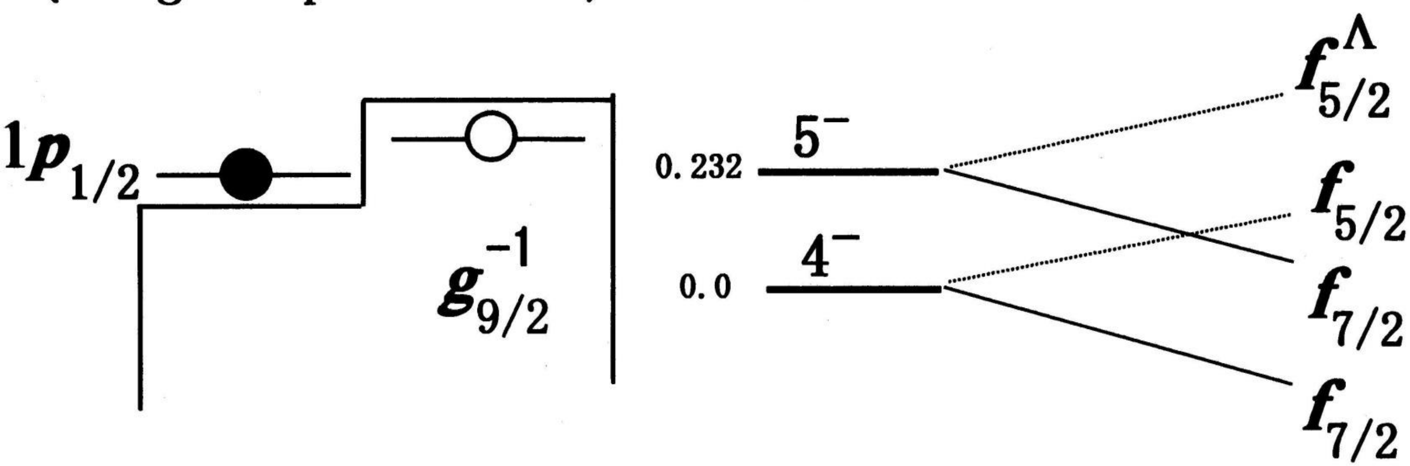

Models for Stucture of $^{89}_{\Lambda}Y$:

Core(J)x hyperon coupling

(3) Many [1p-1h] $_{J_c}$ multiplets of the ^{88}Y core excitation due to V_{NN}.

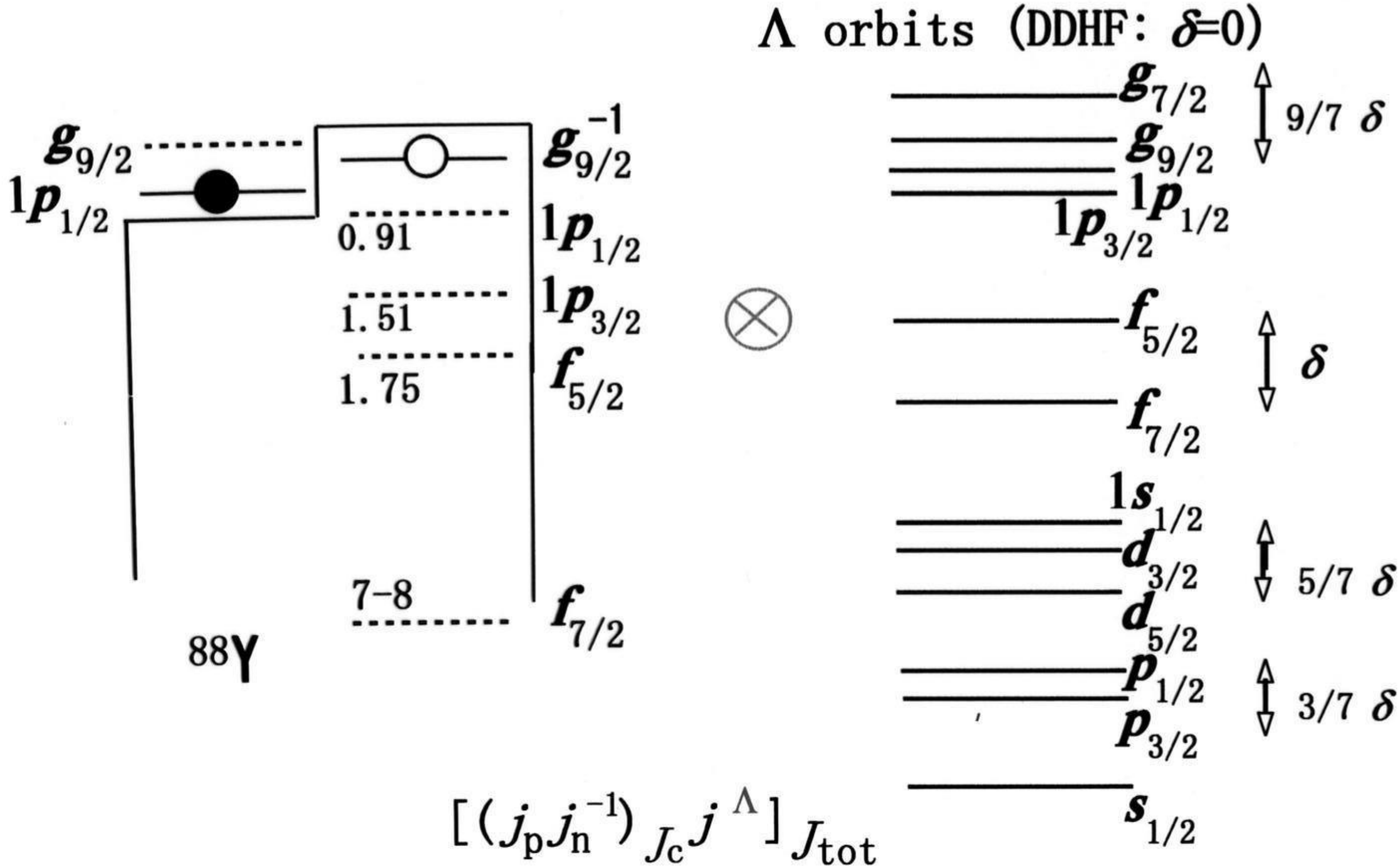

18

All the 2*p*-1*h* configurations adopted

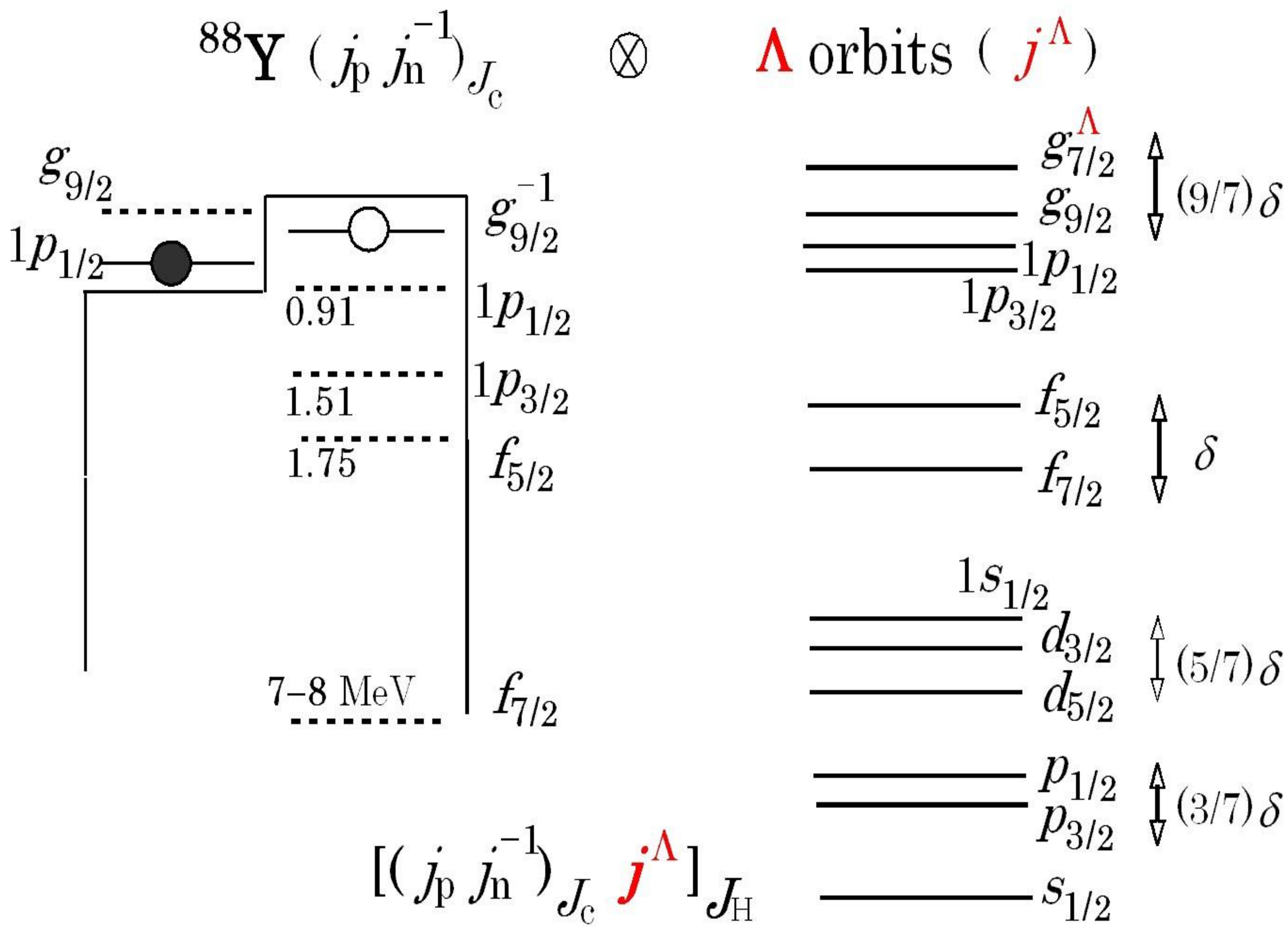

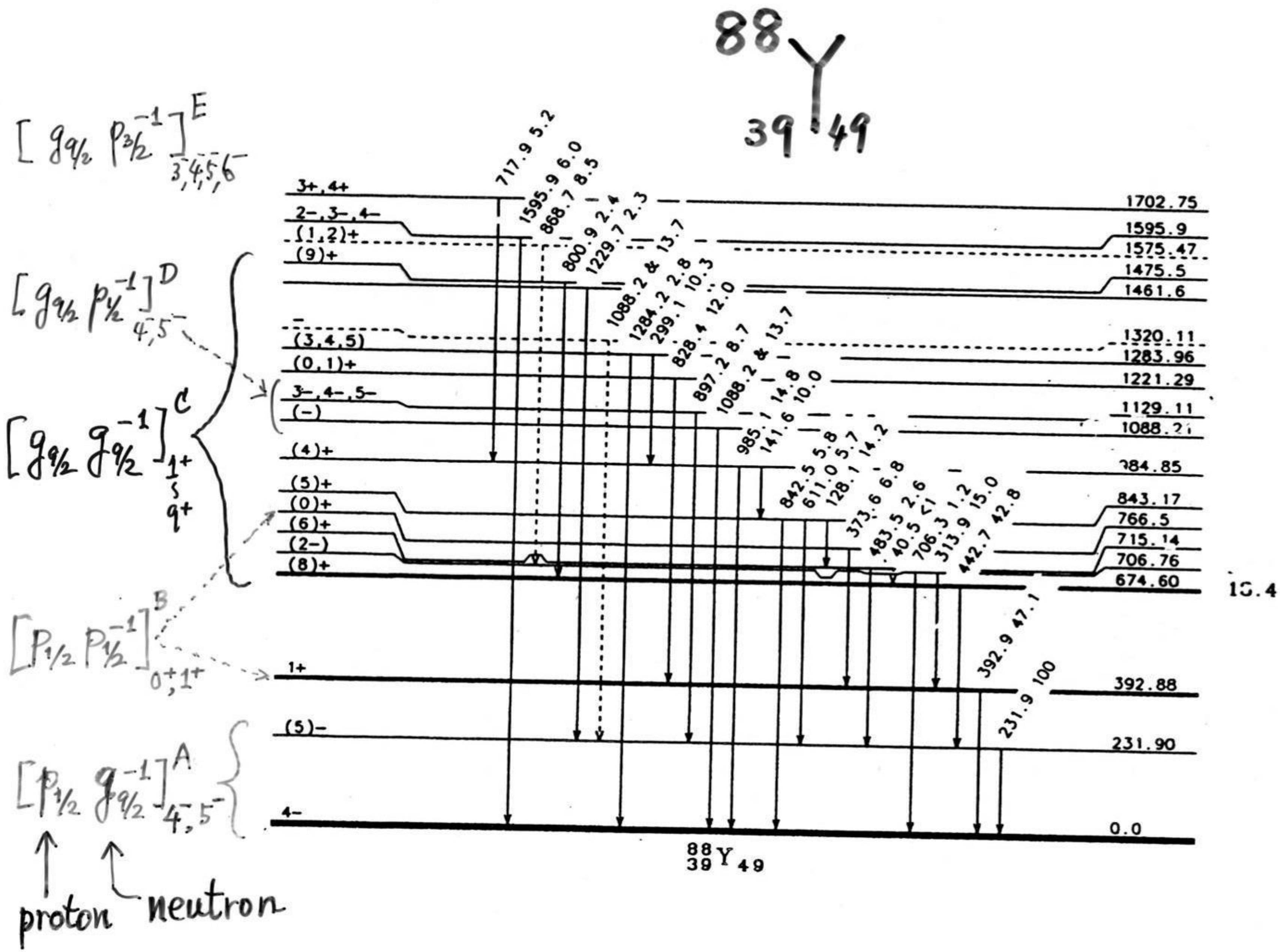

88Y 39 49
[g9/2 p3/2^-1]^E 3,4,5,6
[g9/2 p1/2^-1]^D 4,5−
[g9/2 g9/2^-1]^C 1+ ... 9+
[p1/2 p1/2^-1]^B 0+,1+
[p1/2 g9/2^-1]^A 4,5−
proton
neutron
1702.75
1595.9
1575.47
1475.5
1461.6
1320.11
1283.96
1221.29
1129.11
1088.21
984.85
843.17
766.5
715.14
706.76
674.60
392.88
231.90
0.0

Eigenvalues E(J) and each major configuration

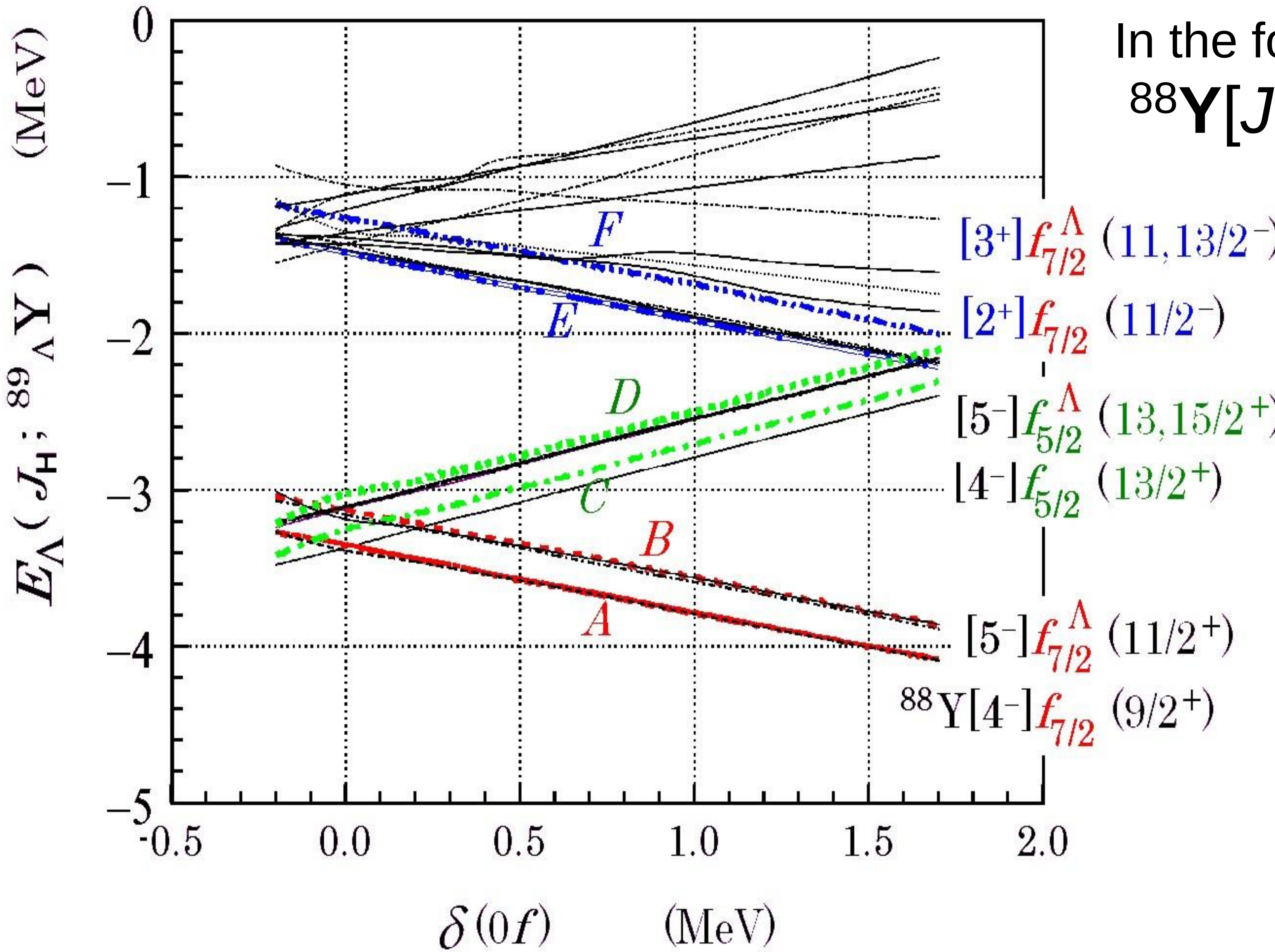

In the form of
$^{88}\mathbf{Y}[J_c]\ .\ j^{\Lambda}$

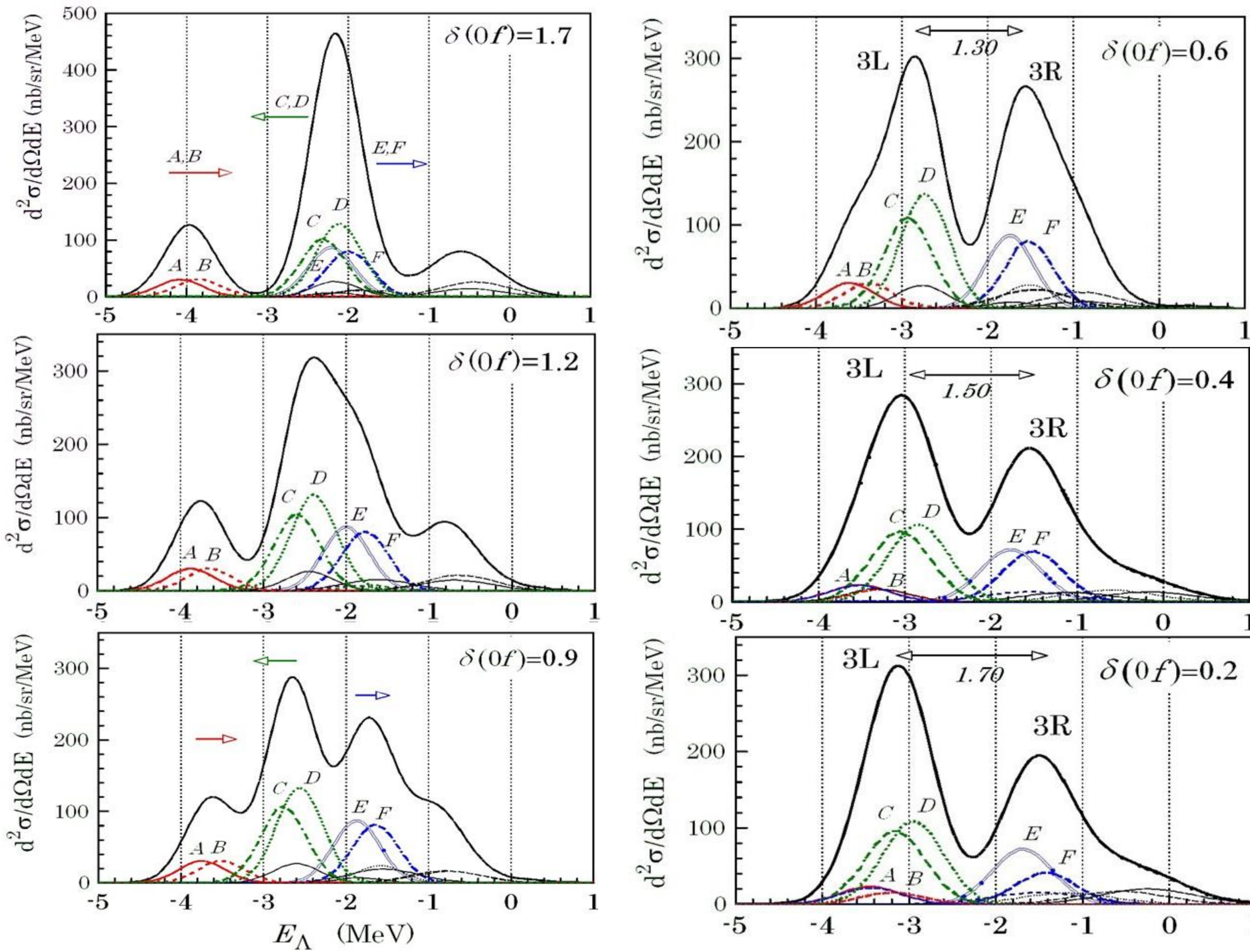
δ(0f)=1.7
δ(0f)=1.2
δ(0f)=0.9
δ(0f)=0.6
δ(0f)=0.4
δ(0f)=0.2
3L
3R
1.30
1.50
1.70
A,B
C,D
E,F
A
B
C
D
E
F
d²σ/dΩdE (nb/sr/MeV)
E_Λ (MeV)

Relative peak strengths as a function of $\delta=\varepsilon(f5/2)-\varepsilon(f7/2)$

Doublet 2L-2R peaks

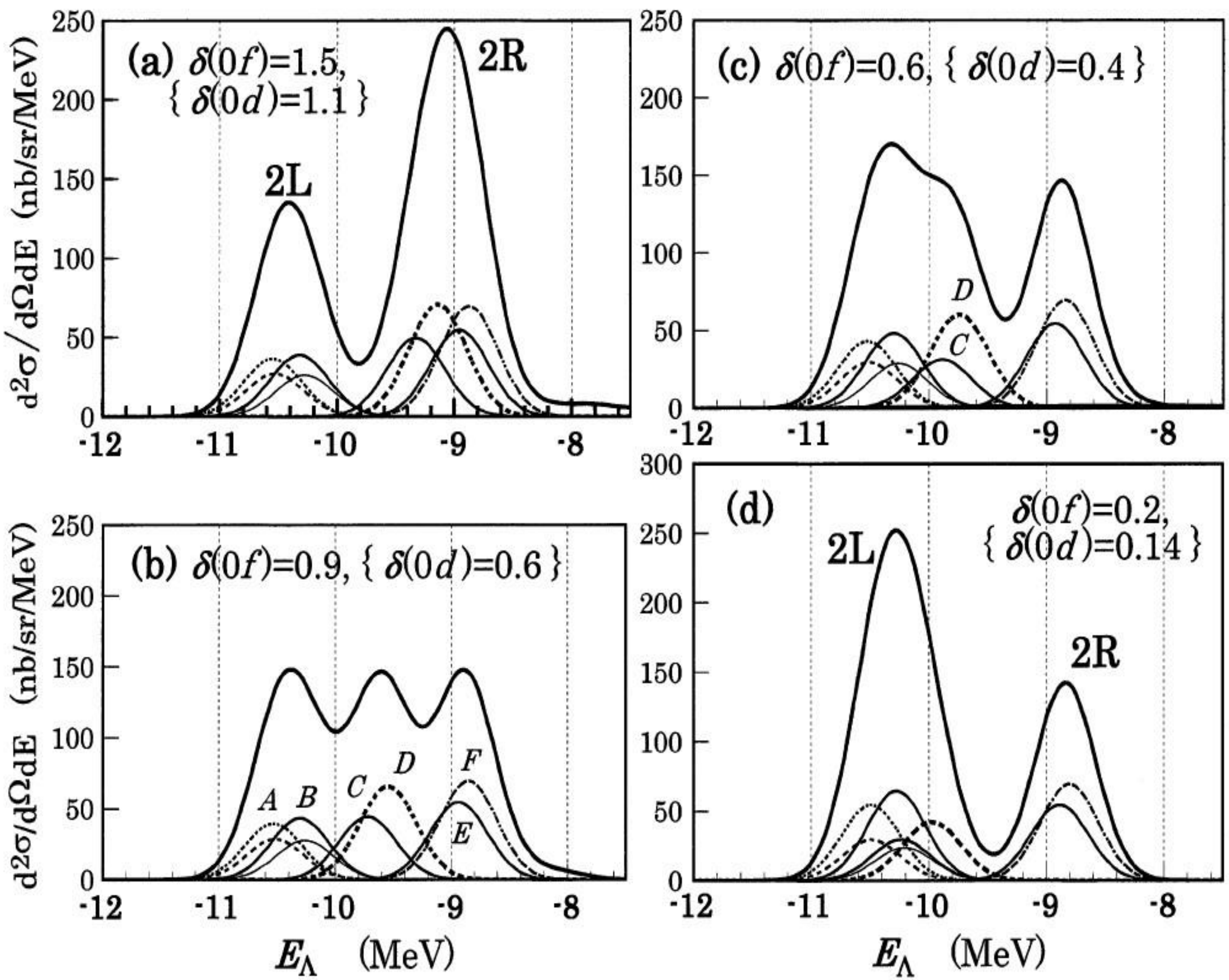

best value
$\delta(0f)=0.2$
$\delta(0d)=0.14$
MeV

Consistent results with data from ${}^{13}_{\Lambda}C$.

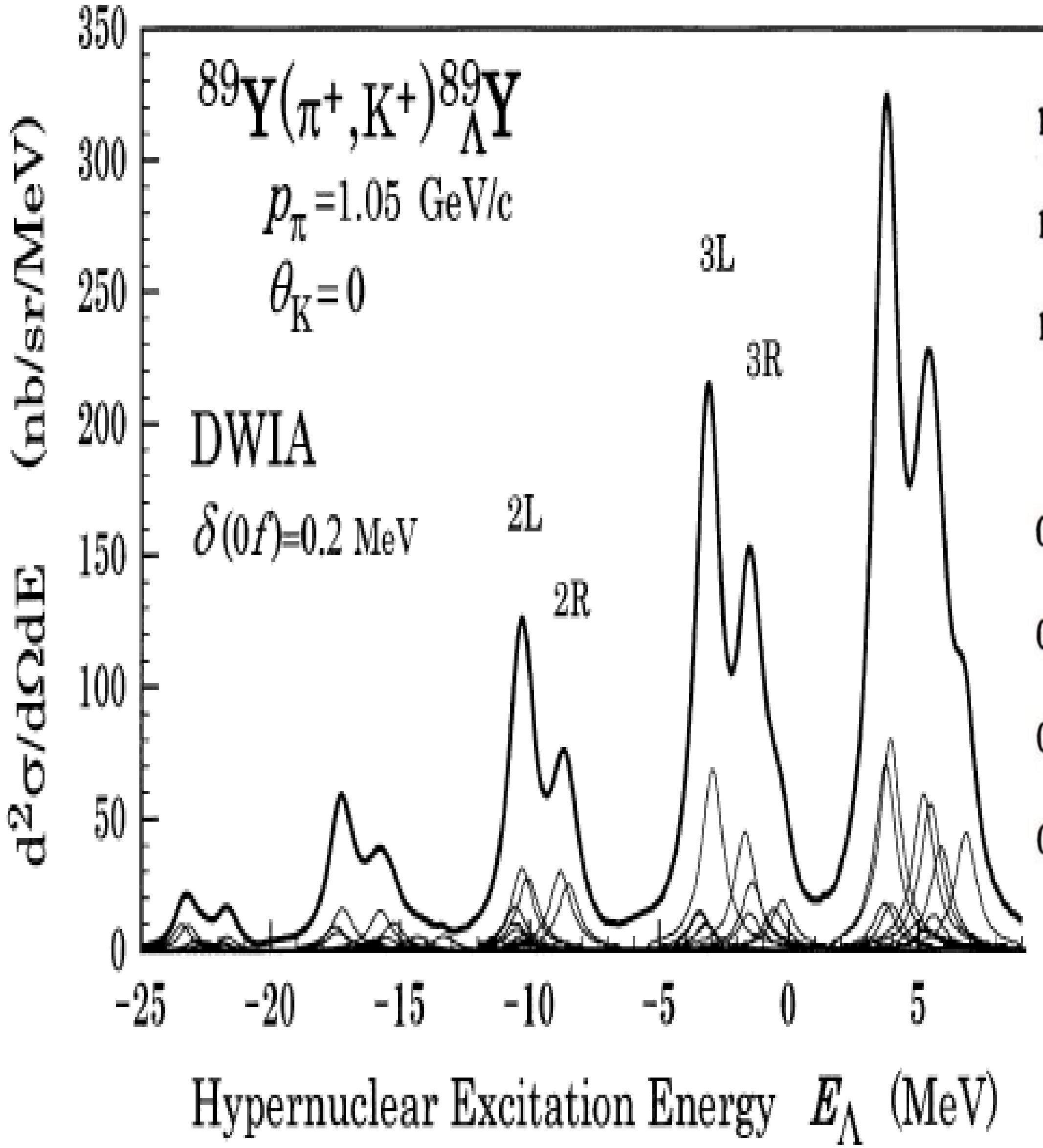

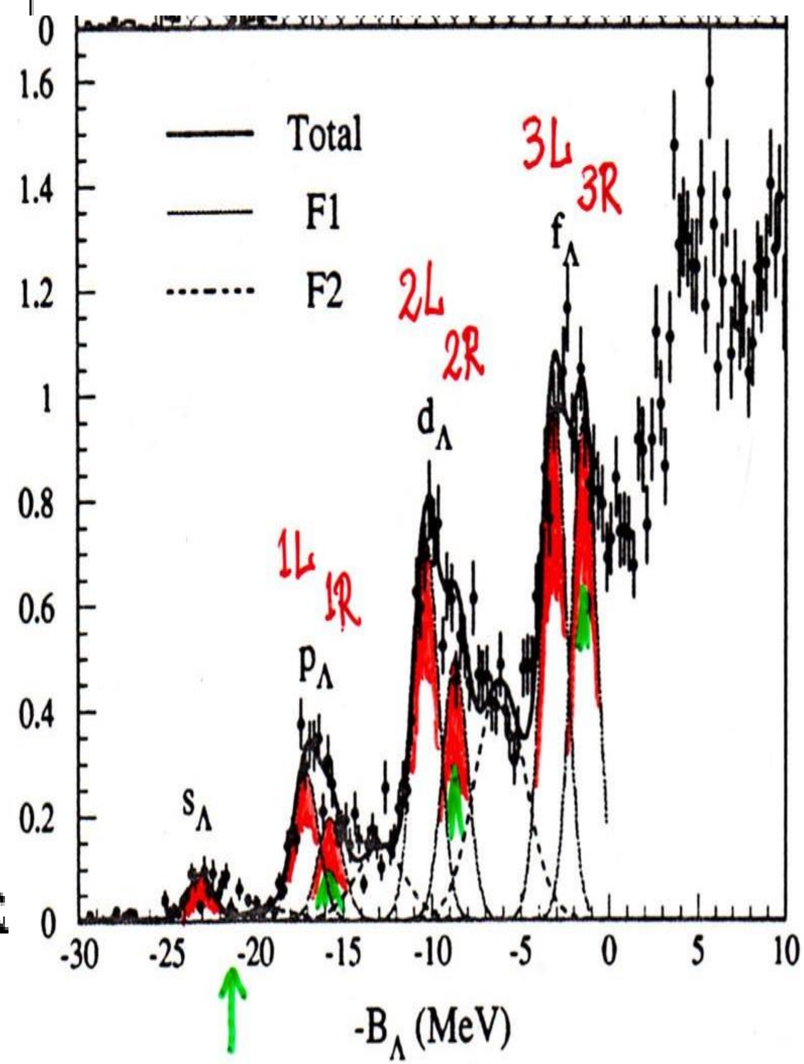

Both f7/2 and f5/2 orbits are in the “3L” peak, while the “3R” peak is subpeak series based on the core-excitation.

Prediction of meson theoretical ΛN potentials

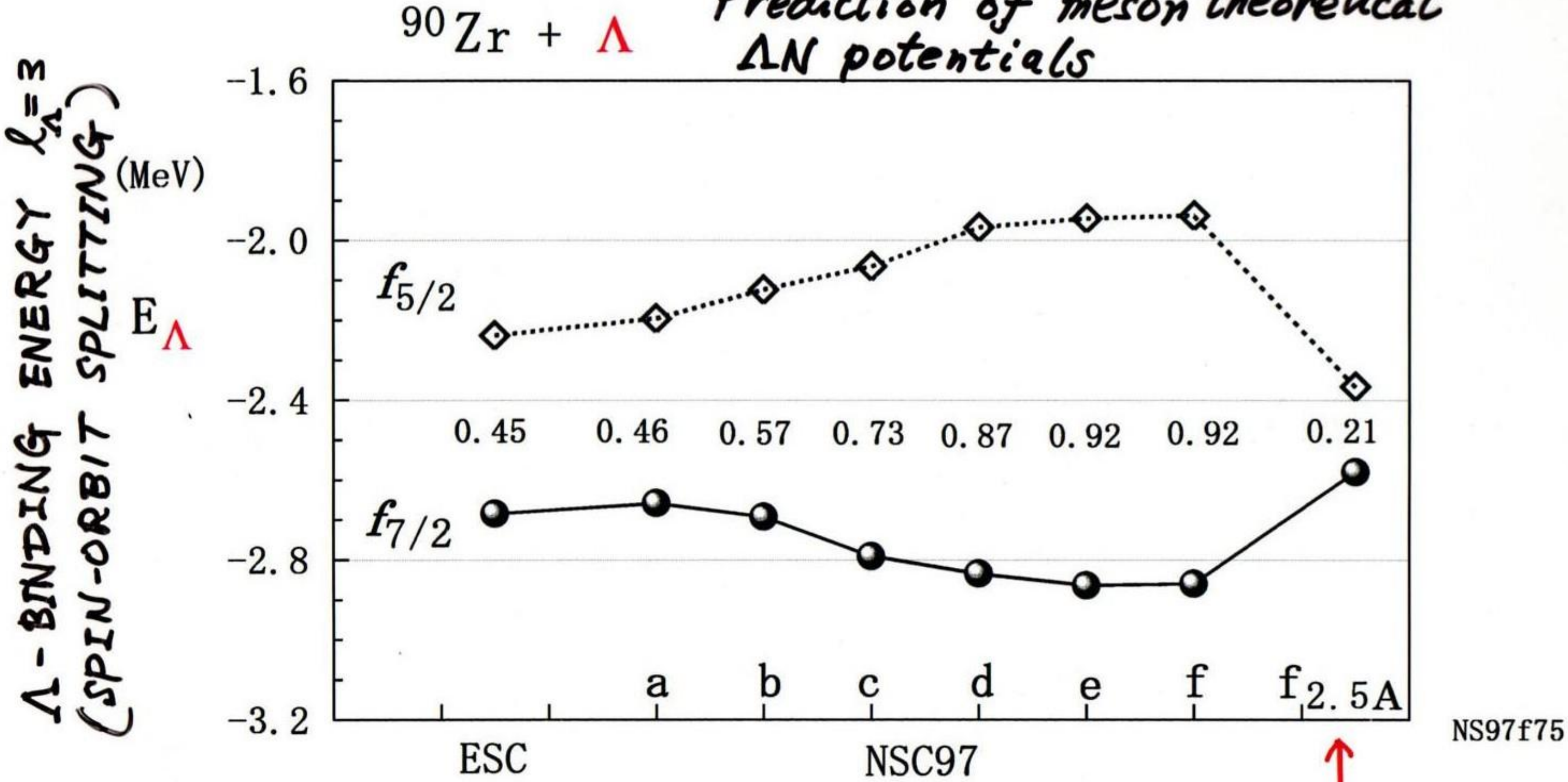

NSC97's give several times larger spin-orbit splittings than the exp. data of $^{9}_{\Lambda}$Be and $^{13}_{\Lambda}$C as disclosed recently.

LS + 2.5ALS
(consistent with Exp. $^{9}_{\Lambda}$Be, $^{13}_{\Lambda}$C splittings)

(3) Interplay of a hyperon with nuclear core dynamics

(a) Deformed core (Rotation $0^+,2^+,4^+$…) x Λ(*nlj*)

Sm isotopes (spherical→deformed)

(b) $^{9}_{\Lambda}$Be → Appearance of "genuinely hypernuclear states"

(New symmetric state [5](50) in SU3) which are forbidden in ordinary nuclei due to the Pauli principle.

Lowering of $p_{//}$ state due to the nuclear core deformation

(c) $^{13}_{\Lambda}$C case as an example of the "spherical core"

3(a) Deformed core (Rotation $0^+,2^+,4^+$...) x Λ(*nlj*)
Sm isotopes (spherical→deformed)

$^{144\text{-}154}_{64}Sm_{82\text{-}90}$

H. Mei, K. Hagino, J.M. Yao, T. Motoba
P.R. C96,014308 (2017)

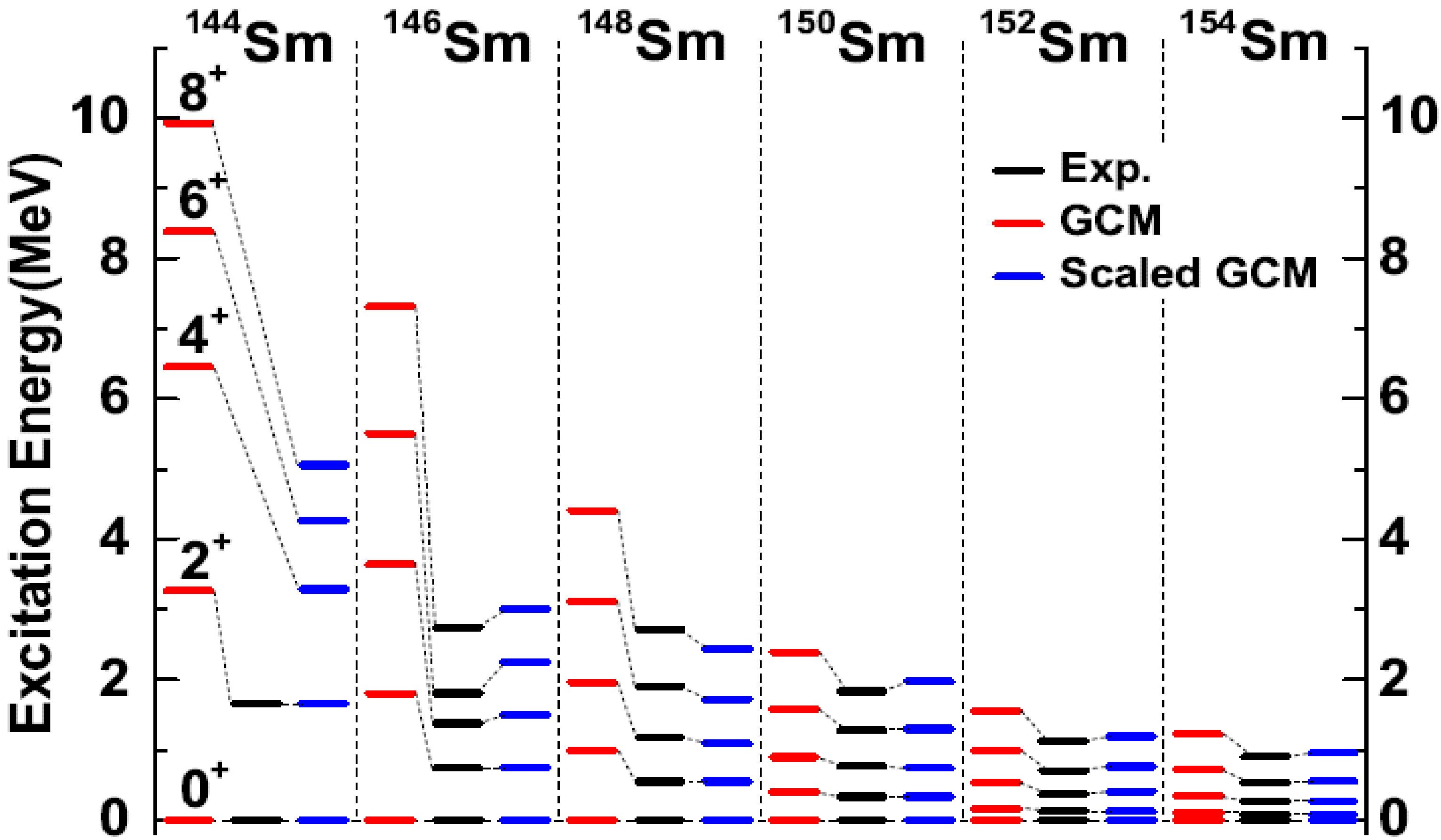

FIG. 2. The yrast levels of the Sm isotopes calculated with the MR-CDFT (the red lines) in comparison to the experiment data (the black lines) taken from Ref. [24]. The figure also shows the scaled levels (the blue lines) with a multiplicative factor of $f = E^{\text{exp.}}_{2^+}/E^{\text{MR-CDFT}}_{2^+}$, that is $E^{\text{Scaled}}_{I^+} = f \cdot E^{\text{MR-CDFT}}_{I^+}$.

$^{144-154}{}_{64}Sm_{82-90}$ isotopes

Total energy as a function of intrinsic quadrupole deformation β

Transition from spherical to deformed characters

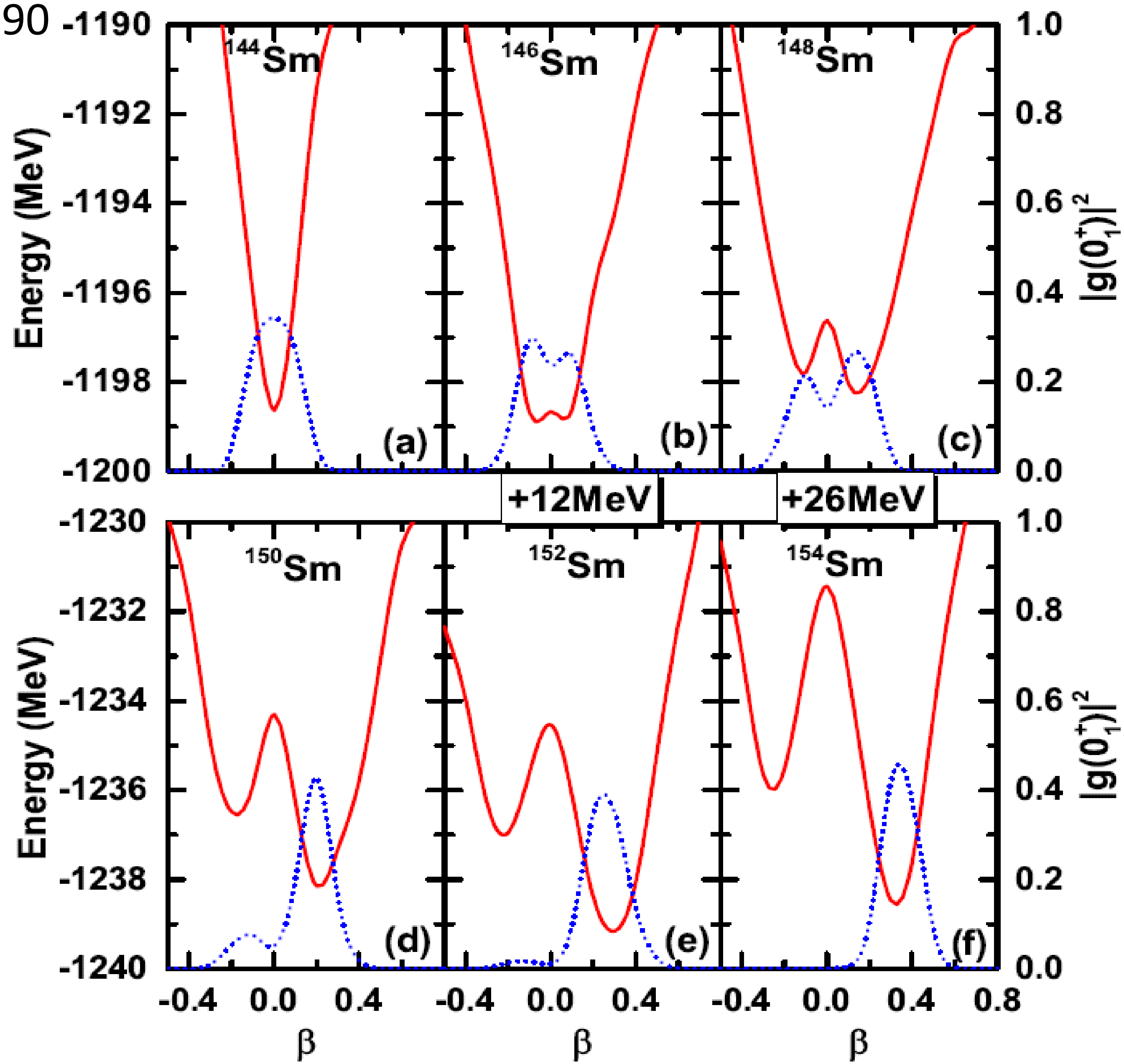

Calculated **E**(4+)/**E**(2+)

B(E2; 2+ → 0+)

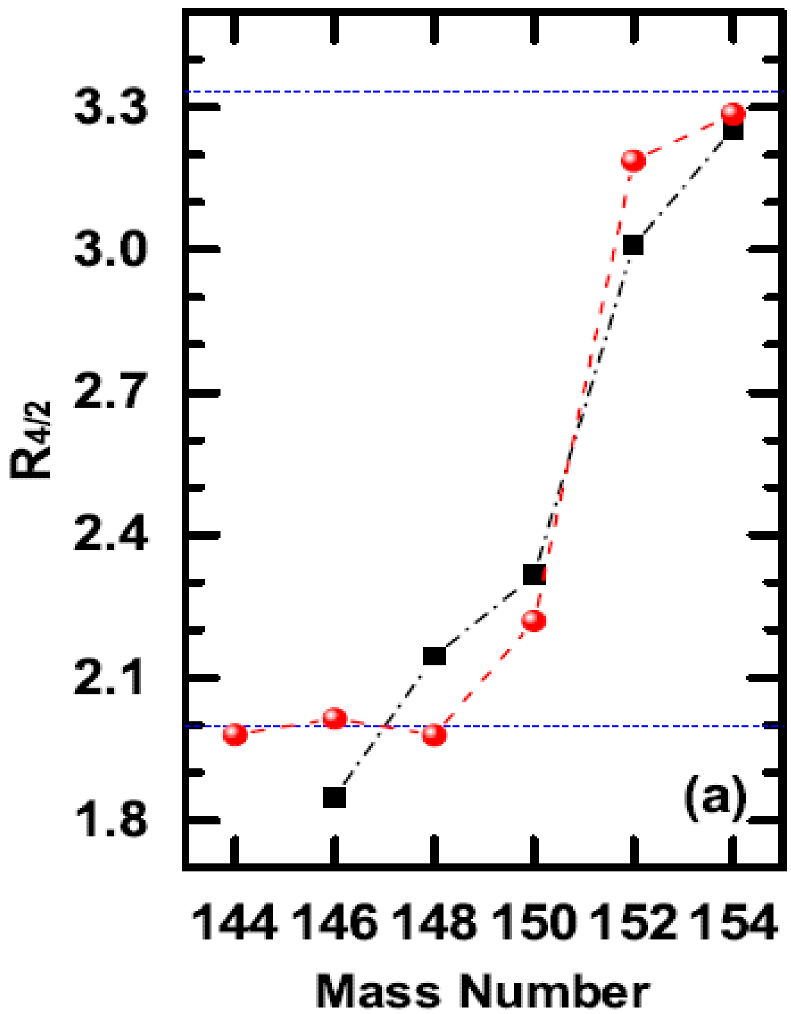

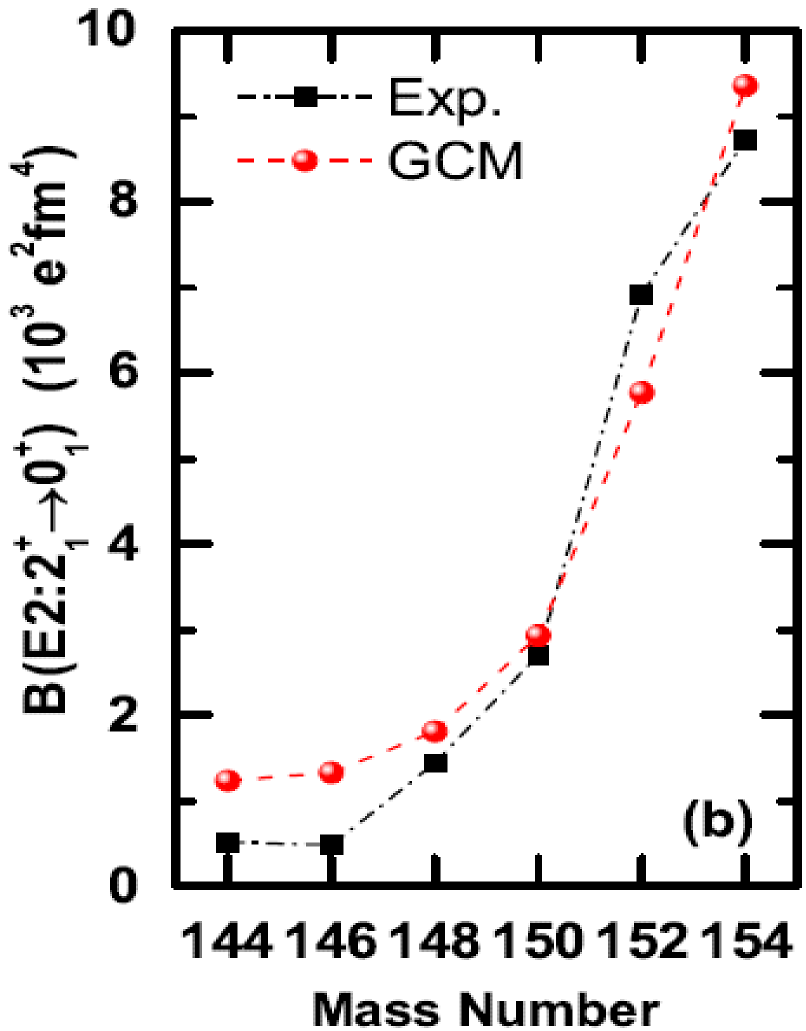

Vibration (spherical) --→ Rotation (deformed)

Relative $B(E2)_{CAL}$: band structure

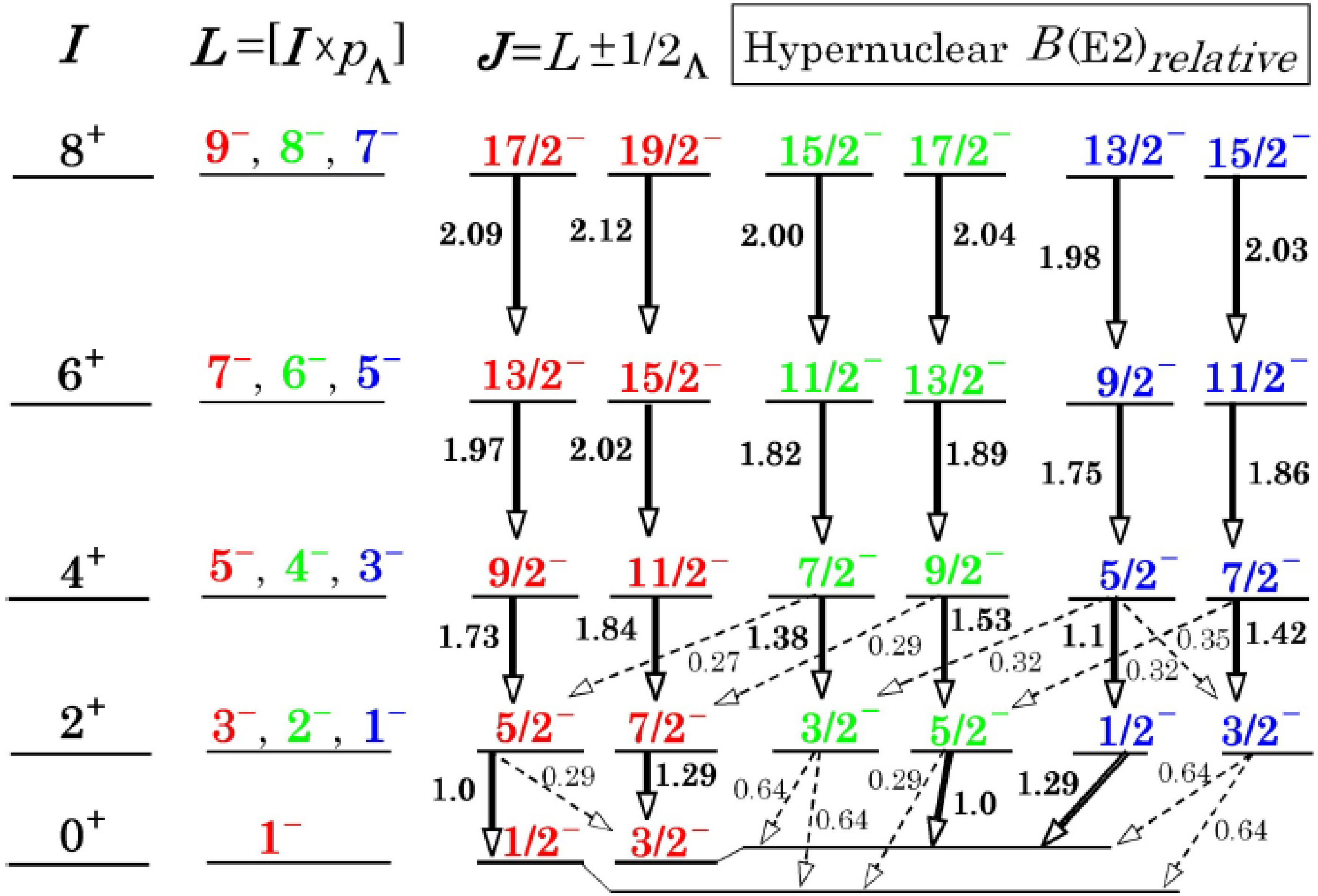

$E(1/2_1^-)$ and $E(3/2_1^-)$ in hypernuclear isotopes

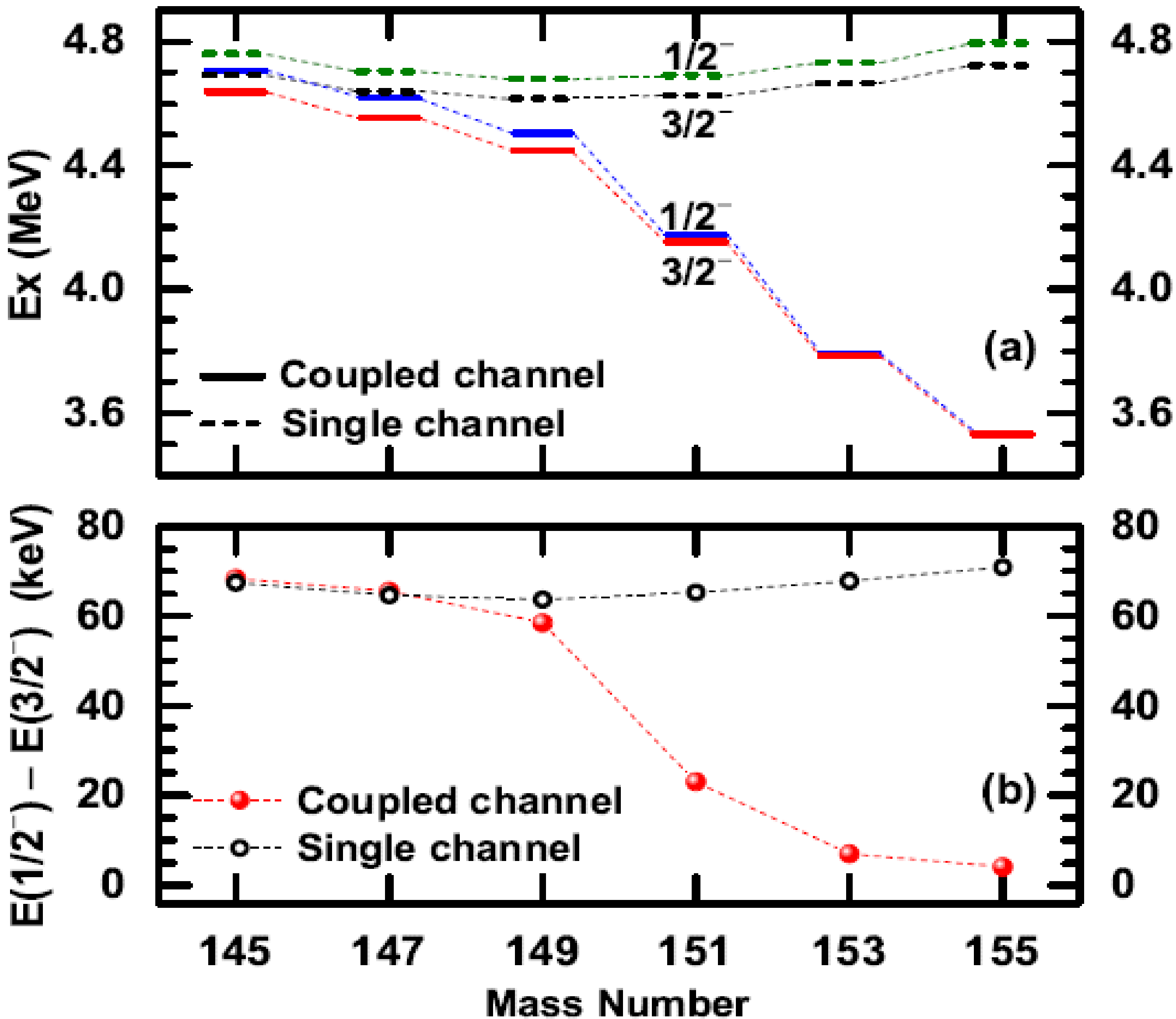

Change of w.f. components in J= $1/2_1^-$, $3/2_1^-$

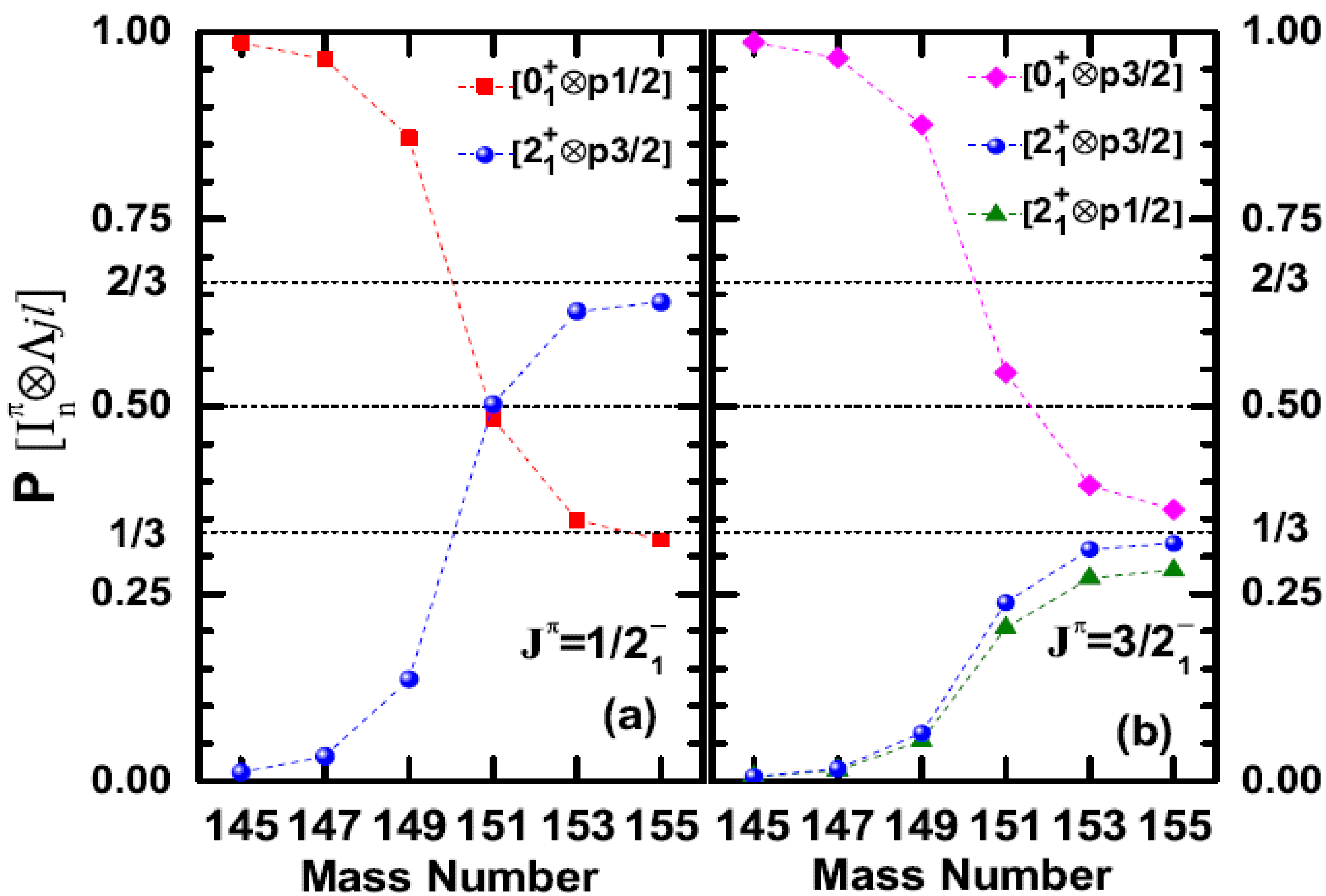

FIG. 8. The probability P_k for the dominant components in the wave function of (a) the $1/2_1^-$ state and (b) the $3/2_1^-$ state as a function of the mass number of the $_\Lambda$Sm isotopes.

WF probability for J^+=[$I \times \Lambda(s_{1/2})$]

positive parity states → weak-coupling: 99%

TABLE I. The probability P of the dominant components, defined as $P \equiv \int dr r^2 |\mathscr{R}_{j\ell nI}(r)|^2$, in the wave functions for the positive-parity states.

J^π	$(lj) \otimes I_n^\pi$	$^{145}_{\Lambda}$Sm	$^{147}_{\Lambda}$Sm	$^{149}_{\Lambda}$Sm	$^{151}_{\Lambda}$Sm	$^{153}_{\Lambda}$Sm	$^{155}_{\Lambda}$Sm
$1/2_1^+$	$s_{1/2} \otimes 0_1^+$	0.998	0.998	0.997	0.994	0.988	0.982
$3/2_1^+$	$s_{1/2} \otimes 2_1^+$	0.997	0.997	0.996	0.993	0.988	0.982
$5/2_1^+$	$s_{1/2} \otimes 2_1^+$	0.997	0.997	0.996	0.993	0.988	0.982
$7/2_1^+$	$s_{1/2} \otimes 4_1^+$	0.991	0.996	0.996	0.993	0.987	0.982
$1/2_2^+$	$s_{1/2} \otimes 0_2^+$	0.987	0.983	0.993	0.992	0.987	0.990
$3/2_2^+$	$s_{1/2} \otimes 2_2^+$	0.981	0.996	0.995	0.992	0.986	0.989
$5/2_2^+$	$s_{1/2} \otimes 2_2^+$	0.980	0.996	0.995	0.991	0.986	0.989
$7/2_2^+$	$s_{1/2} \otimes 4_2^+$	0.988	0.993	0.994	0.987	0.985	0.986

Negative parity state W.F.(J_1^-) vs. deformation

TABLE II. Same as Table I, but for the negative-parity states shown in Fig. 5. The blank entries indicate the probabilities smaller than 0.001.

Spherical core → → deformed

J^π	$(lj) \otimes I_n^\pi$	$^{145}_{\Lambda}$Sm	$^{147}_{\Lambda}$Sm	$^{149}_{\Lambda}$Sm	$^{151}_{\Lambda}$Sm	$^{153}_{\Lambda}$Sm	$^{155}_{\Lambda}$Sm
$1/2_1^-$	$p_{1/2} \otimes 0_1^+$	0.986	0.964	0.859	0.484	0.348	0.322
	$p_{3/2} \otimes 2_1^+$	0.012	0.033	0.136	0.503	0.627	0.639
$3/2_1^-$	$p_{1/2} \otimes 2_1^+$	0.006	0.015	0.054	0.204	0.271	0.281
	$p_{3/2} \otimes 0_1^+$	0.986	0.965	0.876	0.545	0.395	0.363
	$p_{3/2} \otimes 2_1^+$	0.006	0.017	0.064	0.238	0.309	0.318
$5/2_1^-$	$p_{1/2} \otimes 2_1^+$	0.980	0.959	0.573	0.453	0.385	0.346
	$p_{3/2} \otimes 4_1^+$	0.012	0.034	0.154	0.377	0.462	0.504
	$p_{3/2} \otimes 2_1^+$			0.262	0.156	0.127	0.112
$7/2_1^-$	$p_{1/2} \otimes 4_1^+$	0.008	0.022	0.074	0.183	0.232	0.258
	$p_{3/2} \otimes 2_1^+$	0.980	0.954	0.854	0.653	0.554	0.497
	$p_{3/2} \otimes 4_1^+$	0.006	0.018	0.062	0.150	0.188	0.207
$9/2_1^-$	$p_{1/2} \otimes 4_1^+$	0.843	0.931	0.570	0.481	0.398	0.372
	$p_{3/2} \otimes 4_1^+$	0.071	0.016	0.288	0.210	0.166	0.154
	$p_{3/2} \otimes 6_1^+$	0.040	0.033	0.131	0.295	0.407	0.437

10

Be careful that, only in spherical cases, we can extract hyperon single-particle energies ε(nlj>0s1/2) in good approximation.

3(b) Coupling of different parity core states mediated by hyperon (Umeya+)

$^{10}_{\Lambda}$Be の unnatural parity 状態における配位混合

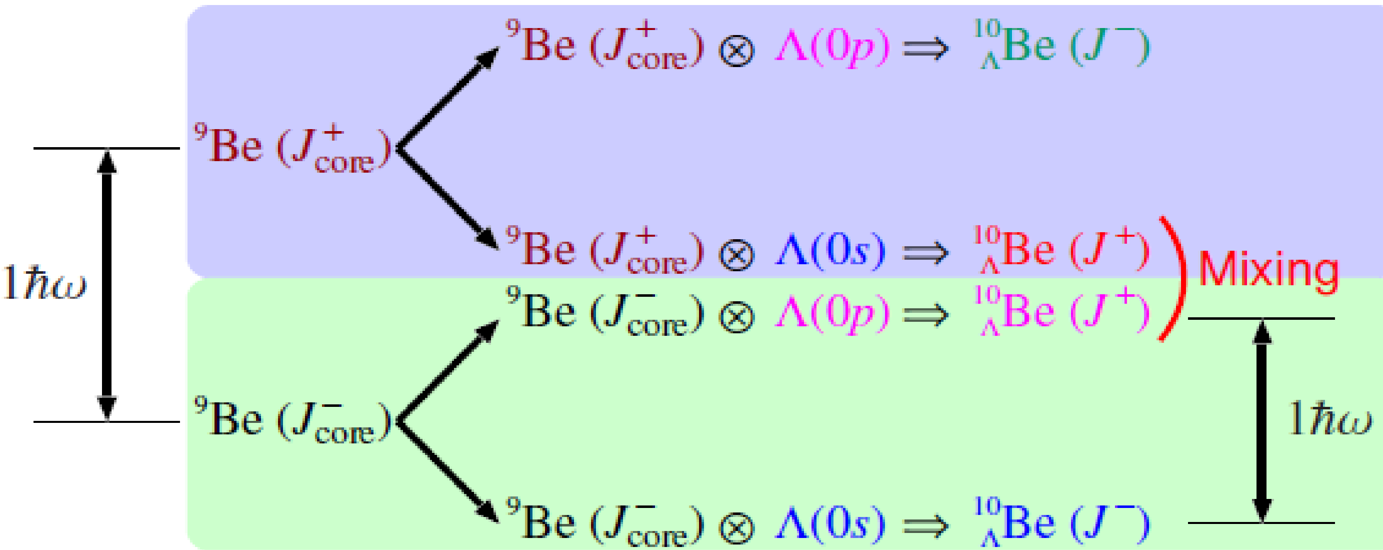

今までの殻模型計算ではコア核は natural parity のみ
$^{10}_{\Lambda}$Be(J^-) は Λ が 0s にいる状態

$^{10}_{\Lambda}$Be(J^+) については　Λ(0s), Λ(0p) のエネルギー差が 1ℏω
^{9}Be(J^-_{core}), ^{9}Be(J^+_{core}) のエネルギー差が 1ℏω

ΛN 相互作用によって コア核が natural parity の状態と
コア核が unnatural parity に励起した状態とが混合する

Parity-mixed multi-configuration Calc. explains the new bump(a), so that the experiment confirms the new symmetric state in ${}^{10}_{\Lambda}$Be for the first time.

結果：^{10}B (γ, K^+) ${}^{10}_{\Lambda}$Be 反応の生成断面積 (2)

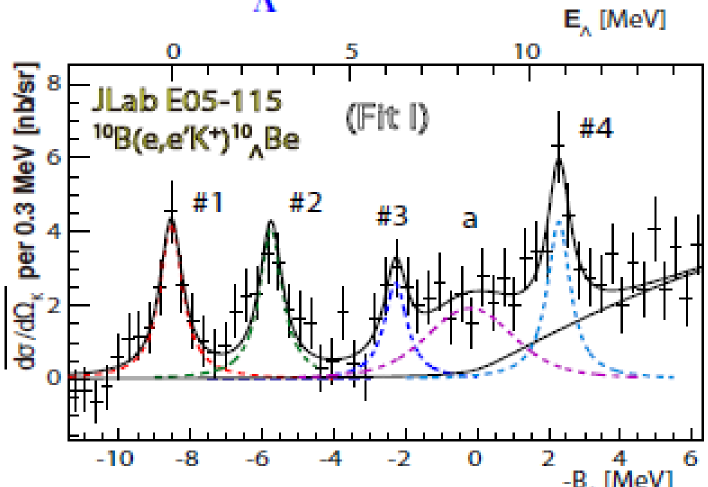

T. Gogami *et al.*,
PRC93, 034314 (2016)

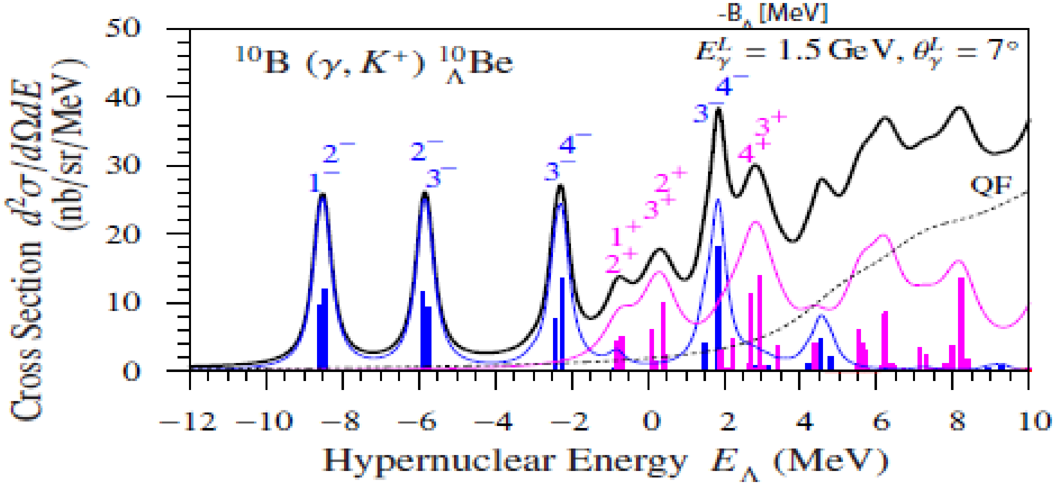

従来の殻模型計算と同様に J^- のピークの計算結果は実験データ#1, #2, #3, #4 とよく一致する

J^+ のいくつかの状態が "a" の部分を作っている

3(c) $^{13}{}_{\Lambda}C$ case as an example of the "spherical core"

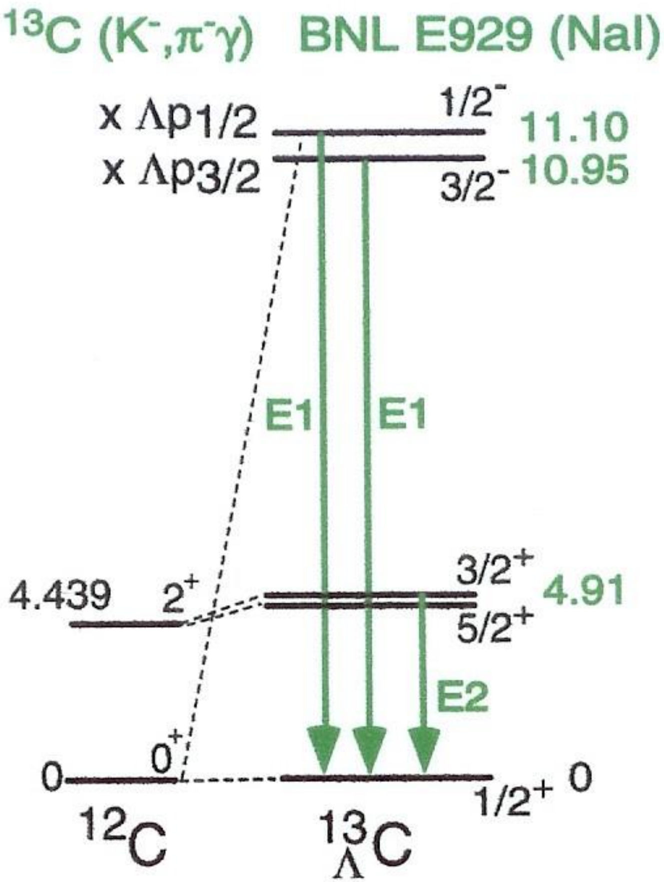

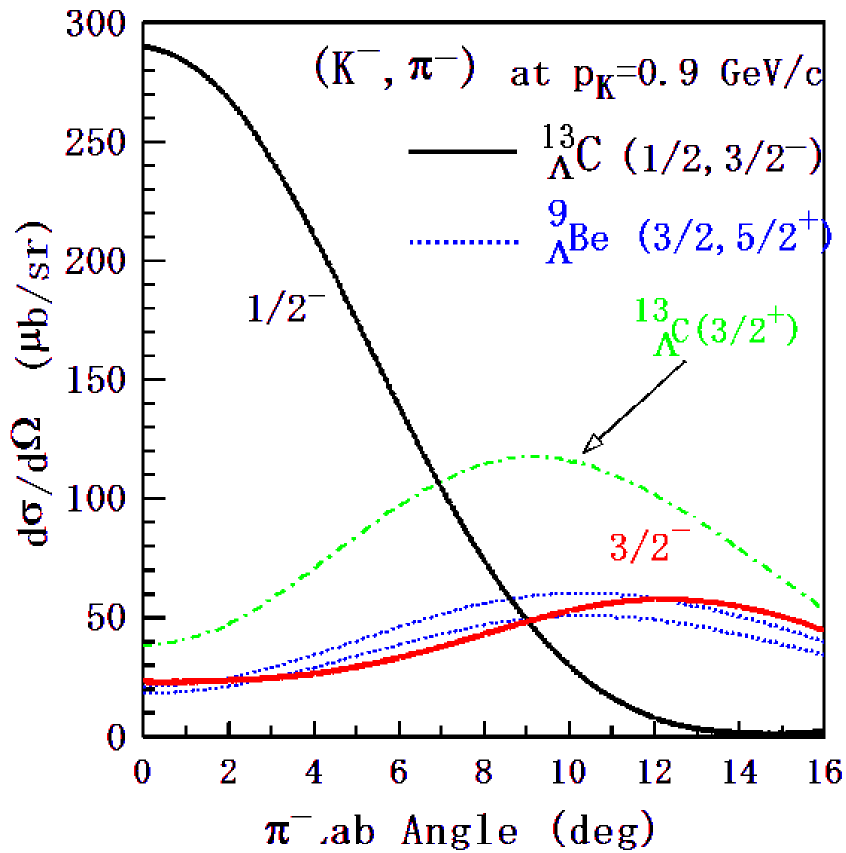

$^{13}{}_{\Lambda}$C case (ref)

Hiyama et al., P.R.L. **85** (2000)

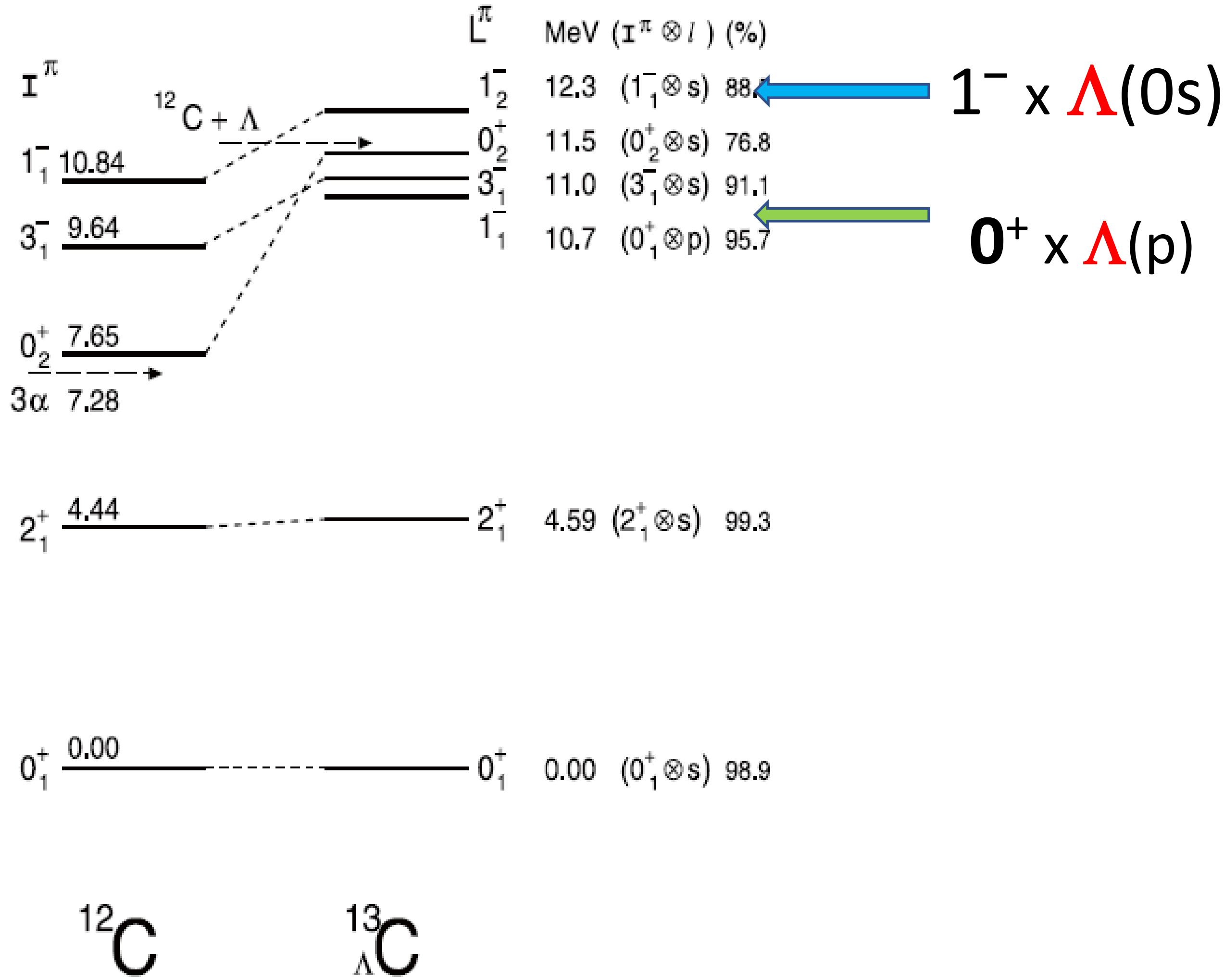

Fig. 5. Calculated excitation energies of $^{13}_{\Lambda}$C with V_0 only (the Λ spin is implicit) compared with the observed excitation energies of ^{12}C. Also shown are the dominant configuration and its percentage contribution. This figure is taken from Ref. 29).

(4) Comments: Suitable (preferable) targets for extracting L single-particle energies

- **"Spherical" targets** or understandable core structures without dense energy levels

- **Couplings with rotational motions** are, of course, quite interesting if they are accessible somehow experimentally in future.

  Deformed target (K-,π-) deformed substitutional states, as in the ^{9}Be(K-,π-) case

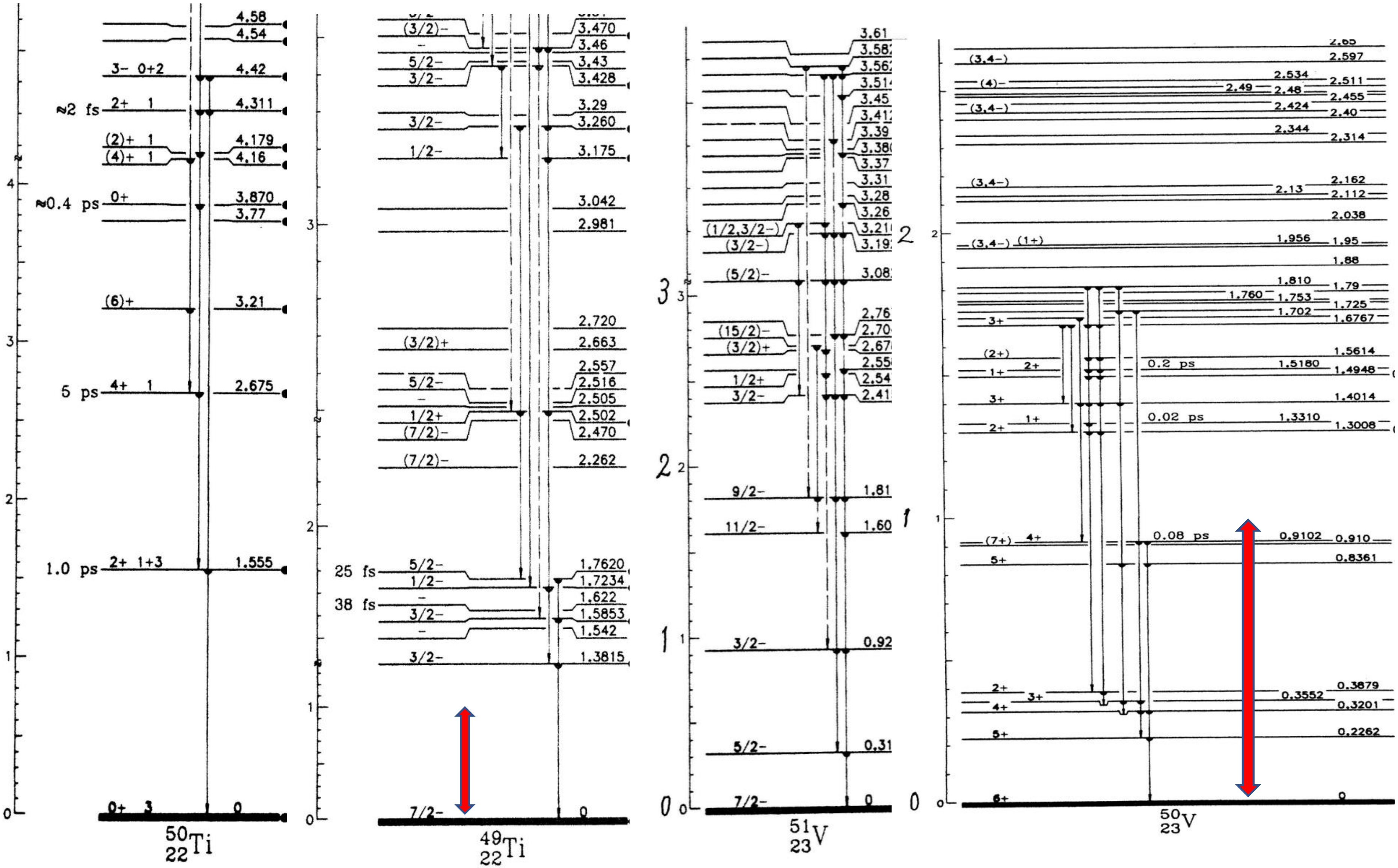

(5.18%)

(99.75%)

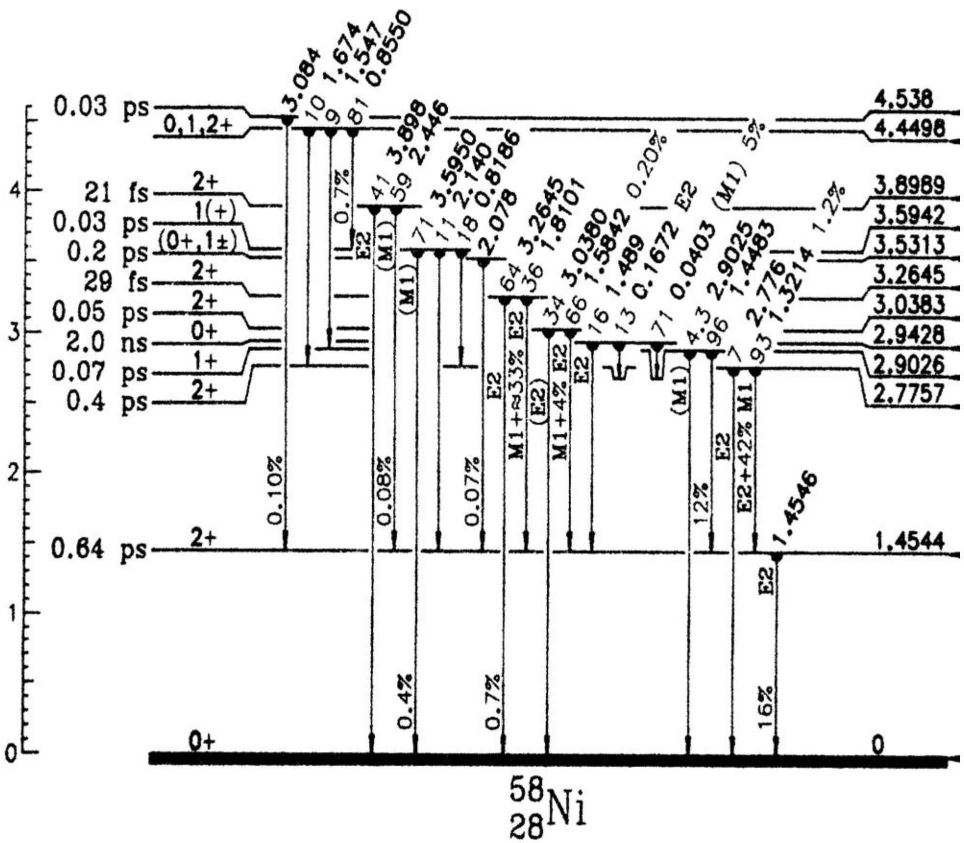

0.03 ps
21 fs
0.03 ps
0.2 ps
29 fs
0.05 ps
2.0 ns
0.07 ps
0.4 ps
0.64 ps
0,1,2+
2+
1(+)
(0+,1±)
2+
2+
0+
1+
2+
2+
0+
4.538
4.4498
3.8989
3.5942
3.5313
3.2645
3.0383
2.9428
2.9026
2.7757
1.4544
0
3.084
1.674
1.547
0.8550
3.898
2.446
3.5950
2.140
0.8186
2.078
3.2645
1.8101
3.0380
1.5842
1.489
0.1672
0.0403
2.9025
1.4483
2.776
1.3214
1.4546
0.10%
0.08%
0.4%
0.07%
0.7%
0.7%
0.20%
(M1) 5%
1.2%
12%
16%
E2
(M1)
M1+≈33%
(E2)
M1+4%
E2+42%
M1
$^{58}_{28}$Ni

(68.08 %)

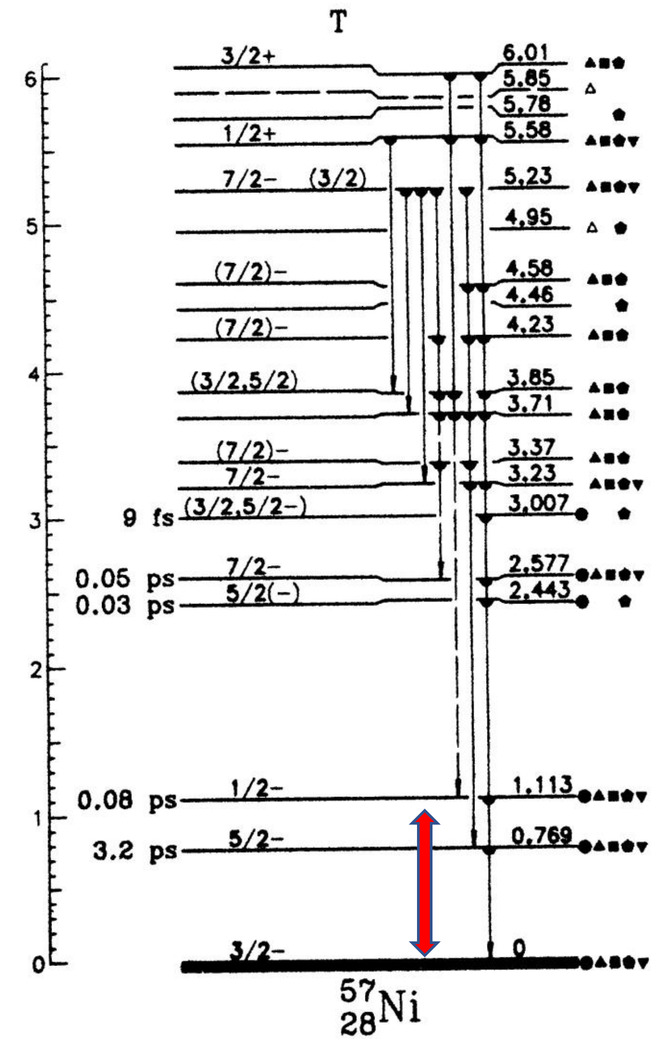

T
3/2+
1/2+
7/2- (3/2)
(7/2)-
(7/2)-
(3/2,5/2)
(7/2)-
7/2-
9 fs (3/2,5/2-)
0.05 ps 7/2-
0.03 ps 5/2(-)
0.08 ps 1/2-
3.2 ps 5/2-
3/2-
6.01
5.85
5.78
5.58
5.23
4.95
4.58
4.46
4.23
3.85
3.71
3.37
3.23
3.007
2.577
2.443
1.113
0.769
0
$^{57}_{28}$Ni

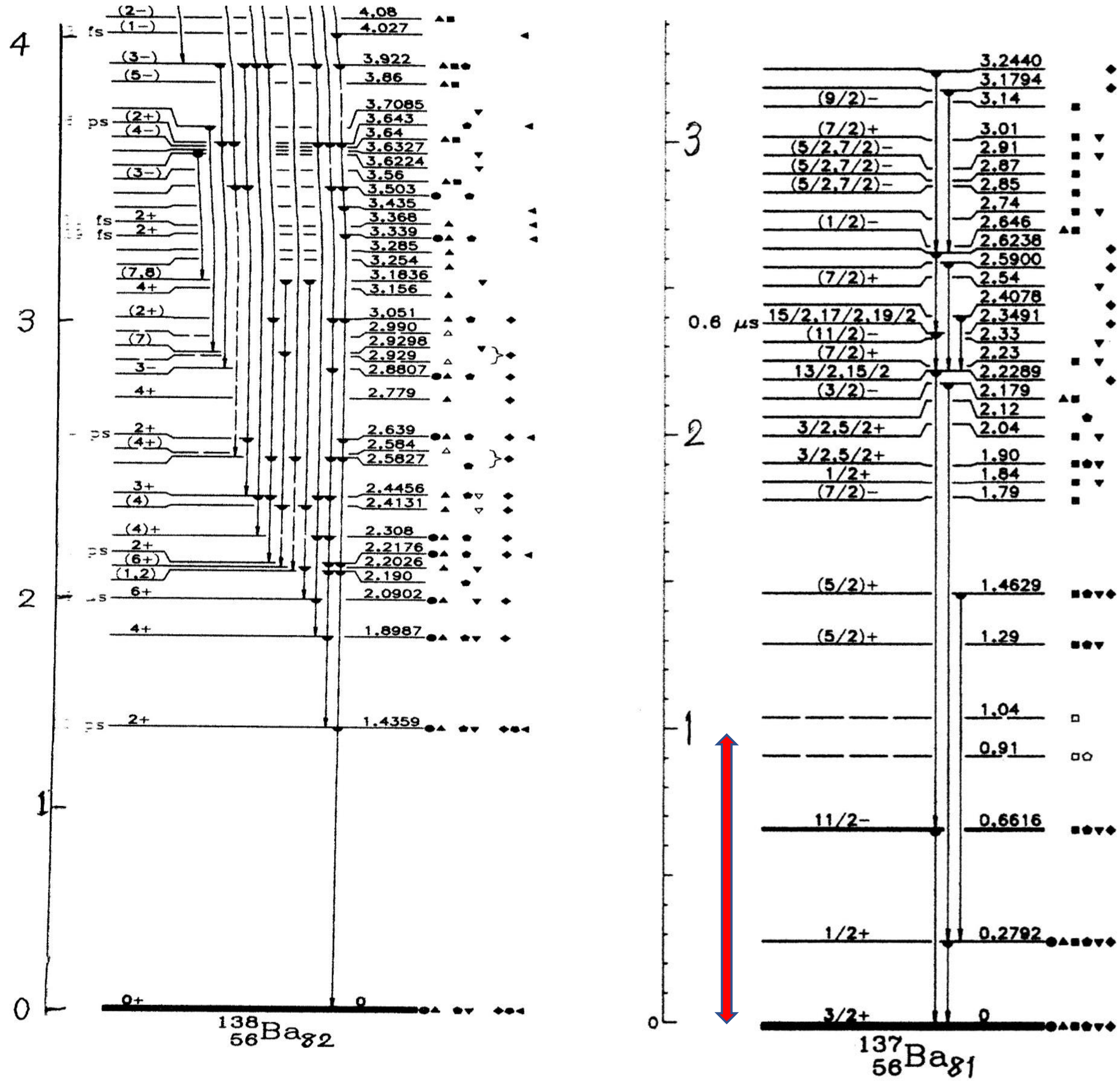

$^{138}_{56}Ba_{82}$
$^{137}_{56}Ba_{81}$
0.6 μs

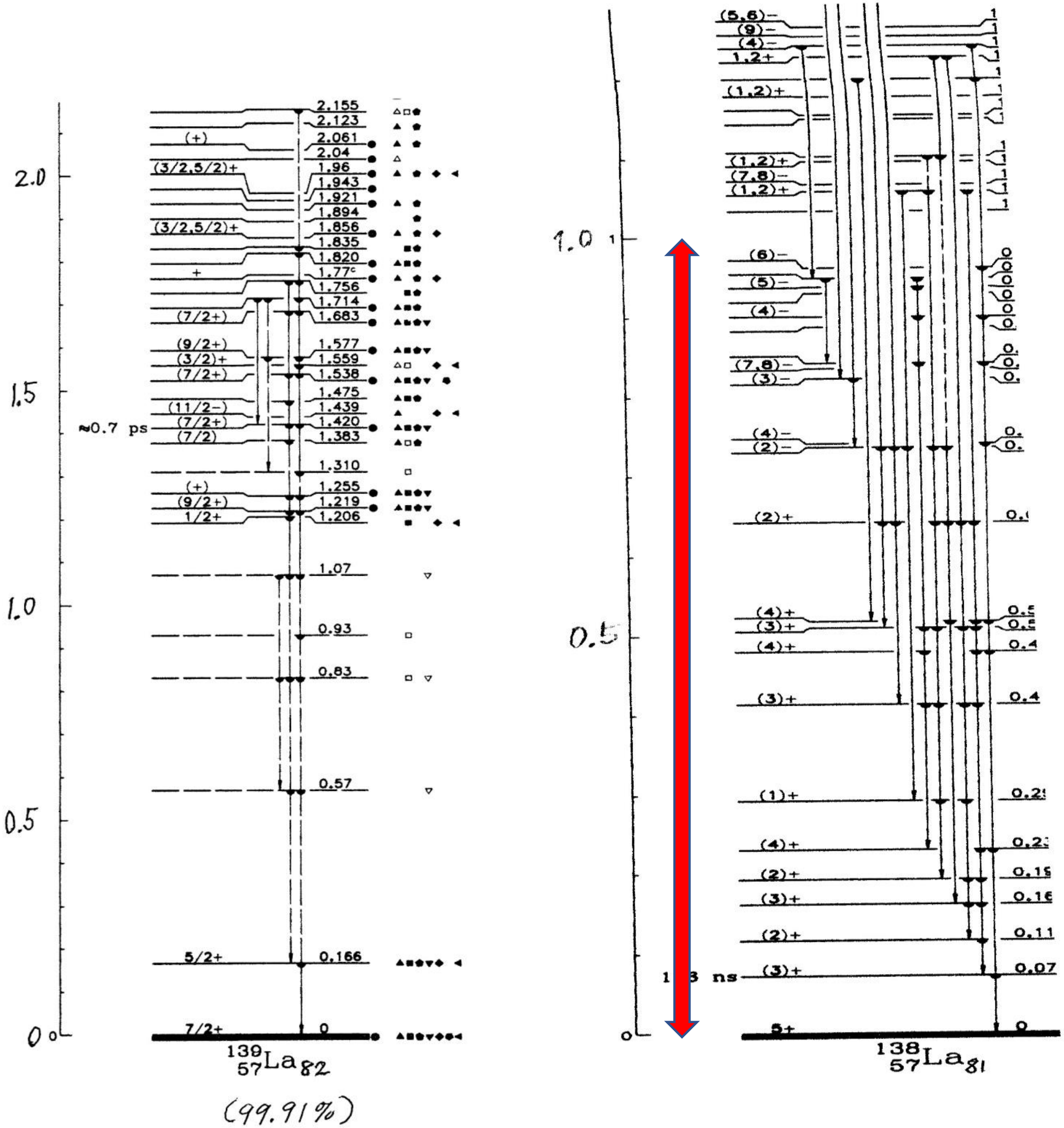
$^{139}_{57}La_{82}$
(99.91%)
≈0.7 ps
$^{138}_{57}La_{81}$
1.0
0.5
0

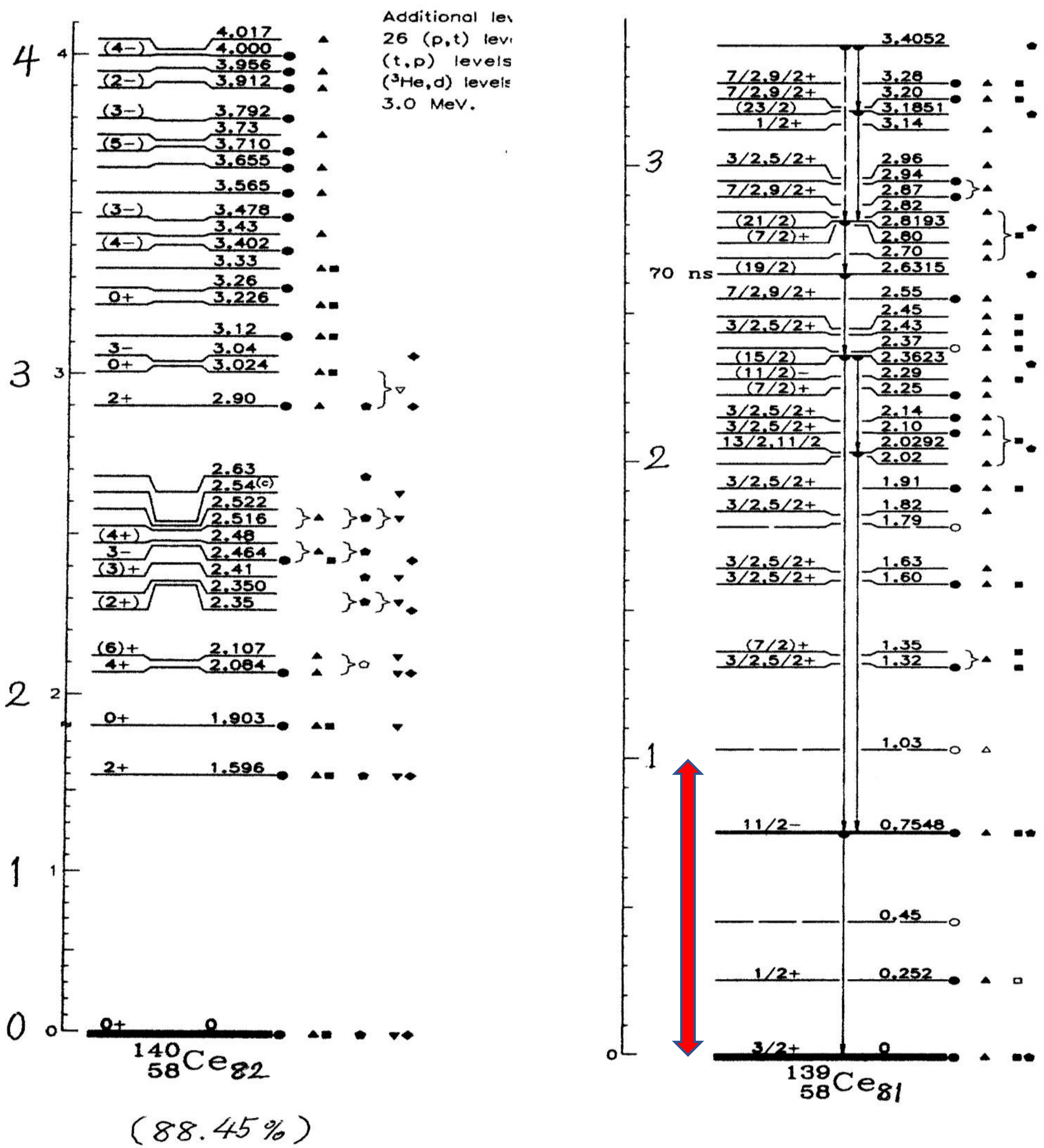
Additional lev
26 (p,t) lev
(t,p) levels
(^{3}He,d) levels
3.0 MeV.
4.017
(4−) 4.000
3.956
(2−) 3.912
(3−) 3.792
3.73
(5−) 3.710
3.655
3.565
(3−) 3.478
3.43
(4−) 3.402
3.33
3.26
0+ 3.226
3.12
3− 3.04
0+ 3.024
2+ 2.90
2.63
2.54(c)
2.522
2.516
(4+) 2.48
3− 2.464
(3)+ 2.41
2.350
(2+) 2.35
(6)+ 2.107
4+ 2.084
0+ 1.903
2+ 1.596
0+ 0
$^{140}_{58}Ce_{82}$
(88.45%)
3.4052
7/2,9/2+ 3.28
7/2,9/2+ 3.20
(23/2) 3.1851
1/2+ 3.14
3/2,5/2+ 2.96
2.94
7/2,9/2+ 2.87
2.82
(21/2) 2.8193
(7/2)+ 2.80
2.70
70 ns (19/2) 2.6315
7/2,9/2+ 2.55
2.45
3/2,5/2+ 2.43
2.37
(15/2) 2.3623
(11/2)− 2.29
(7/2)+ 2.25
3/2,5/2+ 2.14
3/2,5/2+ 2.10
13/2,11/2 2.0292
2.02
3/2,5/2+ 1.91
3/2,5/2+ 1.82
1.79
3/2,5/2+ 1.63
3/2,5/2+ 1.60
(7/2)+ 1.35
3/2,5/2+ 1.32
1.03
11/2− 0.7548
0.45
1/2+ 0.252
3/2+ 0
$^{139}_{58}Ce_{81}$

SUMMARY

(1) Review of the detailed analysis of ^{89}Y(p+,K+)$_{\Lambda}{}^{89}$Y, emphasizing an important role of core-excitations.

(2) Dynamical interplay of L hyperon with nuclear collective motion (deformation)
Examples: Sm isotopes, $_{\Lambda}{}^{9}$Be, $_{\Lambda}{}^{10}$Be $_{\Lambda}{}^{13}$C, etc.

(3) Discussed target candidates suitable to extract Λ s.p.e. in medium/heavy region